

# SARS-CoV-2 Omicron boosting induces de novo B cell response in humans

<https://doi.org/10.1038/s41586-023-06025-4>

Received: 22 September 2022

Accepted: 28 March 2023

Published online: 3 April 2023

 Check for updates

Wafaa B. Alsoussi<sup>1†</sup>, Sameer Kumar Malladi<sup>1†</sup>, Julian Q. Zhou<sup>1</sup>, Zhuoming Liu<sup>2</sup>, Baoling Ying<sup>1,2</sup>, Wooseob Kim<sup>1</sup>, Aaron J. Schmitz<sup>1</sup>, Tingting Lei<sup>1</sup>, Stephen C. Horvath<sup>1</sup>, Alexandria J. Sturtz<sup>1</sup>, Katherine M. McIntire<sup>1</sup>, Birk Evavold<sup>1</sup>, Fangjie Han<sup>3</sup>, Suzanne M. Scheaffer<sup>1,2</sup>, Isabella F. Fox<sup>1</sup>, Senaa F. Mirza<sup>1</sup>, Luis Parra-Rodriguez<sup>4</sup>, Raffael Nachbagauer<sup>5</sup>, Biliana Nestorova<sup>5</sup>, Spyros Chalkias<sup>5</sup>, Christopher W. Farnsworth<sup>1</sup>, Michael K. Klebert<sup>6</sup>, Iskra Pusic<sup>7</sup>, Benjamin S. Strnad<sup>8</sup>, William D. Middleton<sup>8</sup>, Sharlene A. Teeffey<sup>8</sup>, Sean P. J. Whelan<sup>2</sup>, Michael S. Diamond<sup>1,2,4,9,10</sup>, Robert Paris<sup>5</sup>, Jane A. O'Halloran<sup>4,6</sup>, Rachel M. Presti<sup>4,6,9,10</sup>, Jackson S. Turner<sup>1✉</sup> & Ali H. Ellebedy<sup>1,9,10✉</sup>

The primary two-dose SARS-CoV-2 mRNA vaccine series are strongly immunogenic in humans, but the emergence of highly infectious variants necessitated additional doses and the development of vaccines aimed at the new variants<sup>1–4</sup>. SARS-CoV-2 booster immunizations in humans primarily recruit pre-existing memory B cells<sup>5–9</sup>. However, it remains unclear whether the additional doses induce germinal centre reactions whereby re-engaged B cells can further mature, and whether variant-derived vaccines can elicit responses to variant-specific epitopes. Here we show that boosting with an mRNA vaccine against the original monovalent SARS-CoV-2 mRNA vaccine or the bivalent B.1.351 and B.1.617.2 (Beta/Delta) mRNA vaccine induced robust spike-specific germinal centre B cell responses in humans. The germinal centre response persisted for at least eight weeks, leading to significantly more mutated antigen-specific bone marrow plasma cell and memory B cell compartments. Spike-binding monoclonal antibodies derived from memory B cells isolated from individuals boosted with either the original SARS-CoV-2 spike protein, bivalent Beta/Delta vaccine or a monovalent Omicron BA.1-based vaccine predominantly recognized the original SARS-CoV-2 spike protein. Nonetheless, using a more targeted sorting approach, we isolated monoclonal antibodies that recognized the BA.1 spike protein but not the original SARS-CoV-2 spike protein from individuals who received the mRNA-1273.529 booster; these antibodies were less mutated and recognized novel epitopes within the spike protein, suggesting that they originated from naive B cells. Thus, SARS-CoV-2 booster immunizations in humans induce robust germinal centre B cell responses and can generate de novo B cell responses targeting variant-specific epitopes.

The emergence of SARS-CoV-2 variants with increasing numbers of mutations in the spike (S) protein has decreased the effectiveness of primary series vaccinations and led to a recommendation for booster immunizations in most populations<sup>10–16</sup>. Multiple reports have documented that third-dose booster immunizations based on the ancestral Washington strain (WA1/2020) enhanced antibody responses to the ancestral strain as well as emerging variants of concern and correspondingly increased protective effectiveness<sup>5–8,17–21</sup>. In addition, new vaccines based on circulating variants have been developed to

enhance the ability of induced antibodies to combat such variants. Indeed, recent evidence indicates that a B.1.351 (Beta)-containing booster can generate higher titres of neutralizing antibodies against both B.1.351 and B.1.1.529 (Omicron) BA.1 strains of SARS-CoV-2 compared with a booster based on the original strain alone<sup>22</sup>. Additionally, bivalent boosters encoding the original strain and either the BA.1 or BA.5 subvariant induced broader neutralizing antibody responses than the constituent monovalent vaccines<sup>23</sup>. Whether re-exposure to mRNA vaccines encoding S protein from the original SARS-CoV-2 strain or

<sup>1</sup>Department of Pathology and Immunology, Washington University School of Medicine, St Louis, MO, USA. <sup>2</sup>Department of Molecular Microbiology, Washington University School of Medicine, St Louis, MO, USA. <sup>3</sup>Department of Emergency Medicine, Washington University School of Medicine, St Louis, MO, USA. <sup>4</sup>Division of Infectious Diseases, Department of Internal Medicine, Washington University School of Medicine, St Louis, MO, USA. <sup>5</sup>Moderna, Cambridge, MA, USA. <sup>6</sup>Infectious Disease Clinical Research Unit, Washington University School of Medicine, St Louis, MO, USA. <sup>7</sup>Division of Oncology, Department of Medicine, Washington University School of Medicine, St Louis, MO, USA. <sup>8</sup>Mallinckrodt Institute of Radiology, Washington University School of Medicine, St Louis, MO, USA. <sup>9</sup>Center for Vaccines and Immunity to Microbial Pathogens, Washington University School of Medicine, St Louis, MO, USA. <sup>10</sup>The Andrew M. and Jane M. Bursky Center for Human Immunology and Immunotherapy Programs, Washington University School of Medicine, St Louis, MO, USA. <sup>11</sup>These authors contributed equally: Wafaa B. Alsoussi, Sameer Kumar Malladi. ✉e-mail: [turner.j@wustl.edu](mailto:turner.j@wustl.edu); [ellebedy@wustl.edu](mailto:ellebedy@wustl.edu)

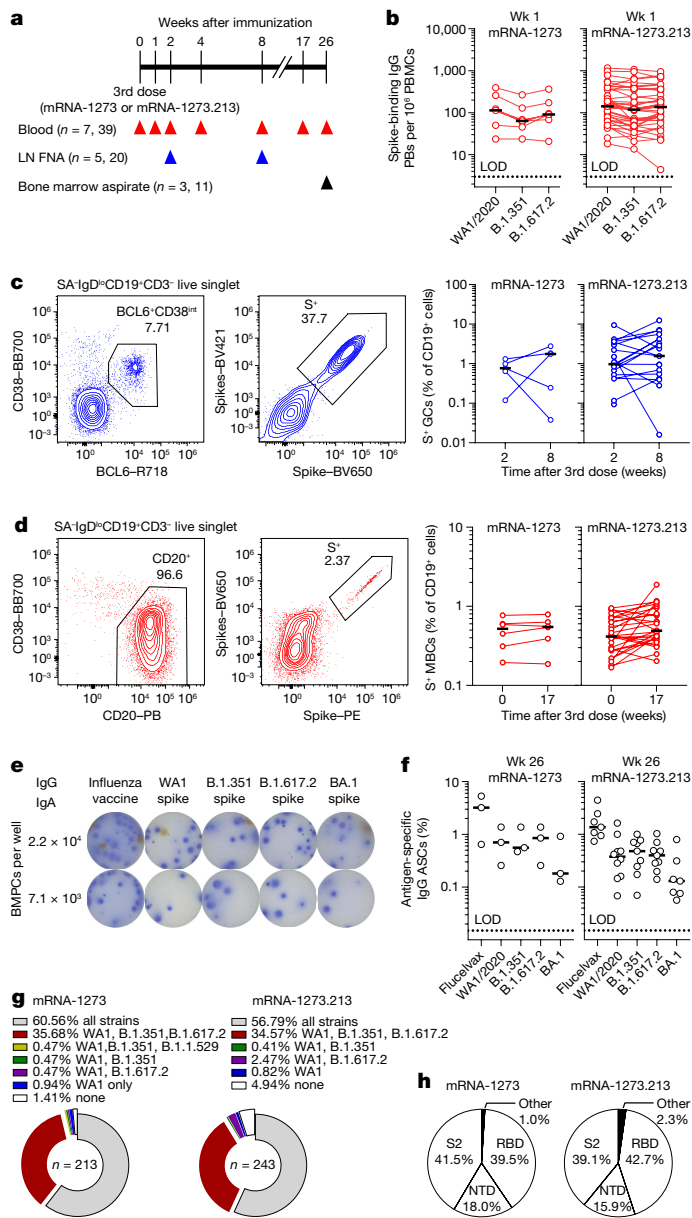


**Fig. 1 | B cell response to mRNA-1273 and mRNA-1273.213 booster immunizations.** **a**, Seven healthy adults received an mRNA-1273 booster and thirty-nine healthy adults received a mRNA-1273.213 booster. Blood was collected at baseline and at 1, 2, 4, 8, 17 and 26 weeks after the booster. FNAs of ipsilateral axillary lymph nodes were collected 2 and 8 weeks after the booster from 5 participants from the mRNA-1273 cohort and from 20 participants from the mRNA-1273.213 cohort; bone marrow aspirates were collected 26 weeks after the booster from 3 participants from the mRNA-1273 cohort and 11 participants from the mRNA-1273.213 cohort. LN, lymph node. **b**, Frequencies of IgG plasmablasts (PBs) specific for the indicated antigens measured by ELISpot in week (wk) 1 PBMCs from participants who received mRNA-1273 (left;  $n = 7$ ) and mRNA-1273.213 (right;  $n = 38$ ). **c, d**, Representative flow cytometry plots of BCL6 and CD38 (**c**) or CD20 and CD38 (**d**) on IgD<sup>lo</sup> B cells in FNA (**c**) or PBMC (**d**) samples (left), pooled (WA1/2020, B.1.351, B.1.617.2 and BA.1) S protein probe (BV421 and BV650) staining on BCL6<sup>+</sup>CD38<sup>int</sup> germinal centre B cells (**c**) and CD20<sup>+</sup>CD38<sup>lo/int</sup> MBCs (**d**) (second from left), and frequencies of S<sup>+</sup> germinal centre B cells from FNA (**c**) or S<sup>+</sup> MBCs from PBMCs (**d**) from participants who received mRNA-1273 (second from right) and mRNA-1273.213 (right). **c**, mRNA-1273,  $n = 5$ ; mRNA-1273.213,  $n = 20$ . **d**, mRNA-1273,  $n = 6$ ; mRNA-1273.213,  $n = 28$ . **e**, Representative ELISpot wells coated with the indicated antigens, developed in blue (IgG) and red (IgA) after plating the indicated numbers of BMPCs. **f**, Frequencies of IgG BMPCs specific for the indicated antigens 26 weeks after participants received mRNA-1273 (left) or mRNA-1273.213 (right) boosters. Lines indicate medians. Symbols at each time point represent one sample. mRNA-1273,  $n = 3$ ; mRNA-1273.213,  $n = 10$ . **g, h**, Binding of monoclonal antibodies from week 17 S<sup>+</sup> MBCs from participants who received mRNA-1273 (left) and mRNA-1273.213 (right) to indicated antigens (**g**) and constituent domains of WA1/2020 S protein (**h**), measured by ELISA.

from variants of concern induce robust germinal centre reactions that are critical for refining high-affinity and durable antibody responses has not been examined in humans. To address this question, we conducted an immunization study of 46 healthy adults with no history of SARS-CoV-2 infection, all of whom had completed a primary two-dose vaccination course with either the Pfizer–BioNTech (BNT162b2) or Moderna (mRNA-1273) SARS-CoV-2 mRNA vaccines, both of which encode a prefusion-stabilized full-length SARS-CoV-2 S protein based on the WA1/2020 strain<sup>24,25</sup>. Recruited individuals received a third booster dose of 50  $\mu$ g mRNA-1273 or mRNA-1273.213, which contains a total of 100  $\mu$ g of mRNA encoding B.1.351 (Beta; sequence conservation of 99.1% for S protein and 98.7% for the receptor binding domain (RBD) compared with WA1/2020) and B.1.617.2 (Delta; sequence conservation of 99.2% for S protein and 99.1% for the RBD compared with WA1/2020) SARS-CoV-2 S proteins (Extended Data Tables 1 and 2), as a sub-study of an ongoing clinical trial (Clinical NCT04927065).

Seven of the participants received a booster immunization of mRNA-1273, and 39 received mRNA-1273.213. Blood samples were collected at baseline and weeks 1, 2, 4, 8, 17 and 26 after vaccination. Five participants from the mRNA-1273 cohort and twenty from the mRNA-1273.213 cohort consented to collection of fine needle aspirates (FNAs) of draining axillary lymph nodes at weeks 2 and 8. Three participants from the

mRNA-1273 cohort and 11 from the mRNA-1273.213 cohort consented to collection of bone marrow aspirates 26 weeks after their third dose (Fig. 1a). Circulating S protein-specific antibody-producing plasmablasts were measured by enzyme-linked immune absorbent spot (ELISpot) assay. S protein-specific IgG- and IgA-producing plasmablasts were detected one week after the booster immunization from all participants in the mRNA-1273 cohort. Robust circulating IgG-producing plasmablast responses against the original WA1/2020 S protein and against the vaccine-encoded B.1.351 and B.1.617.2 S proteins were detected in all participants in the mRNA-1273.213 cohort 1 week after immunization, with lower IgA responses detectable in most participants (Fig. 1b and Extended Data Fig. 1a). Plasma IgG antibody titres against S protein from the WA1/2020, B.1.351, B.1.617.2 and BA.1 strains were measured by multiplex bead binding assay. In both cohorts, plasma antibody binding levels against all strains were increased 4 weeks after immunization and declined approximately 1.3- to 2-fold by 17 weeks (Extended Data Fig. 1b, c).

Ultrasonography was used to identify and guide FNA of accessible axillary lymph nodes on the same side as the site of immunization two and eight weeks after the booster. FNA samples were stained with pooled fluorescently labelled S protein probes from the WA1/2020, B.1.351, B.1.617.2 and BA.1 strains and then analysed by flow cytometry to detect S protein-specific B cells. We included BA.1 S protein probes in the pool to detect memory B cells (MBCs) that may have stochastically mutated to better recognize the variant antigen<sup>26</sup>. Spike-recognizing (S<sup>+</sup>) germinal centre B cells (CD19<sup>+</sup>CD3<sup>+</sup>IgD<sup>lo</sup>BCL6<sup>+</sup>CD38<sup>int</sup>) and follicular helper T (T<sub>FH</sub>) cells (defined as CD3<sup>+</sup>CD19<sup>+</sup>CD4<sup>+</sup>CD8<sup>+</sup>CD14<sup>+</sup>CXCR5<sup>+</sup>PD-1<sup>+</sup>BCL6<sup>+</sup>FOXP3<sup>-</sup>) were detected in FNAs from all participants analysed at week 2. Frequencies of S<sup>+</sup> germinal centre B cells and T<sub>FH</sub> cells correlated significantly and remained readily detectable in all but one participant from each cohort at week 8, consistent with the robust germinal centre response observed after primary vaccination with SARS-CoV-2 mRNA vaccines<sup>2,27,28</sup> (Fig. 1c and Extended Data Fig. 1d–f). Circulating S<sup>+</sup> MBCs in blood were identified as CD19<sup>+</sup>CD3<sup>+</sup>IgD<sup>lo</sup>CD20<sup>+</sup> cells that bound the pooled fluorescently labelled S protein probes. S<sup>+</sup> MBCs were detected in all participants before the booster administration

and at similar frequencies 17 weeks after the booster, with median frequencies of 0.52% and 0.55% of the total circulating B cells in the mRNA-1273 cohort, and 0.42% and 0.49% in the mRNA-1273.213 cohort (Fig. 1d). Consistent with sustained plasma antibody titres, bone marrow plasma cells (BMPCs) producing IgG that bound WA1/2020, B.1.351, B.1.617.2 and BA.1S proteins were detected in all thirteen participants with enough BMPCs for ELISpot (3 from the mRNA-1273 and 10 from the mRNA-1273.213 cohort). Although the differences were not statistically significant, the frequencies of BMPCs that bound WA1/2020, B.1.351 and B.1.617.2 S proteins were approximately half of those of seasonal influenza vaccine-specific BMPCs, which accumulate over a lifetime of repeated antigen exposures. Similarly, the frequencies of BA.1-binding BMPCs were approximately one-quarter of those binding the other strains. S protein-binding IgA-producing BMPCs were considerably rarer or undetectable (Fig. 1e,f and Extended Data Fig. 1g,h).

To characterize the breadth of the MBC repertoire after boosting, we selected three participants from each cohort for whom we had characterized the B cell response to the primary vaccination series: 382-02, 382-07 and 382-08 from the mRNA-1273 cohort and 382-01, 382-13 and 382-15 from the mRNA-1273.213 cohort<sup>2,29</sup>. For both cohorts, we stained week 17 post-boost peripheral blood mononuclear cells (PBMCs) with pooled fluorescently labelled S protein probes from the WA1/2020, B.1.351, B.1.617.2 and BA.1 strains, enabling us to sort MBCs for monoclonal antibody generation independently of the S protein probe that they bound. We also bulk-sorted week 17 total MBCs for heavy chain immunoglobulin sequencing to broaden the clonal repertoire analyses (Extended Data Fig. 2a and Extended Data Table 3). We generated 81, 59, 73, 94, 90 and 59 clonally distinct monoclonal antibodies from participants 382-02, 382-07, 382-08, 382-01, 382-13 and 382-15, respectively. We next assessed the binding of these antibodies to S protein from the WA1/2020, B.1.351, B.1.617.2 and BA.1 strains by enzyme-linked immunosorbent assay (ELISA). In total, 205 out of 213 (96%) and 222 out of 243 (91%) monoclonal antibodies derived from the MBCs from the mRNA-1273 and mRNA-1273.213 cohorts, respectively, recognized the original WA1/2020, B.1.351 and B.1.617.2 S proteins, with 129 (61%) and 138 (57%), respectively, also recognizing BA.1 (Fig. 1g). Evaluation of the domains targeted by each monoclonal antibody revealed that 40%, 18% and 42% from the mRNA-1273 cohort and 43%, 16% and 39% from the mRNA-1273.213 cohort bound RBD, the N-terminal domain (NTD) and S2, respectively (Fig. 1h).

To track the clonal dynamics of the B cell response in the two cohorts, we performed single-cell RNA sequencing (scRNA-seq) on week 1 sorted plasmablasts and week 2 and week 8 FNA specimens from the same 6 participants and bulk-sorted germinal centre B cells and lymph node plasma cells (LNPCs) for heavy chain immunoglobulin sequencing (Fig. 2a,e, Extended Data Fig. 3a–g and Extended Data Tables 3–5). We then computationally inferred clonal relationships on the basis of common heavy chain V and J gene usage, CDR3 lengths and CDR3 similarity<sup>30,31</sup> to link the B cell receptor sequences to known S-specific clones identified among monoclonal antibodies derived from MBCs isolated 17 weeks after the third vaccine dose or from the previously characterized response to the primary vaccination series<sup>2,29</sup> (Fig. 2b,e, Extended Data Fig. 3h and Extended Data Table 6). The majority of S-specific plasmablasts identified by scRNA-seq after the booster dose were clonally related to MBCs, germinal centre B cells and/or plasma cells induced by primary vaccination (Fig. 2c). Multiple S-specific clones were detected in the plasmablast response after both the second dose of the primary vaccination series and the booster. Representatives of these clones participating in the booster plasmablast response had significantly higher somatic hypermutation (SHM) frequencies in their immunoglobulin heavy chain variable region (IGHV) genes than those from the primary response, consistent with their recall from affinity-matured MBCs (Fig. 2d). S-specific plasmablast clones identified one week after the booster dose were identified in germinal centre responses in all six analysed participants, although the peak frequencies of the S-specific

germinal centre clonal repertoire occupied by plasmablast clones varied from 17% to 100% among participants (Extended Data Fig. 3i,j). SHM frequencies among S-specific MBCs isolated 17 weeks after the booster were significantly higher than their clonally related counterparts isolated 6 months after the primary vaccination, consistent with additional rounds of germinal centre-driven maturation (Fig. 2f). Similar trends were observed among paired S-specific BMPC clones analysed 6 or 9 months after the primary immunization and 6 months after the booster. However, SHM did not increase in all clonal families, consistent with durable populations of MBCs and BMPCs generated by the primary vaccine response persisting through the booster response (Fig. 2f,g). mRNA-1273 and mRNA-1273.213 both elicited robust germinal centre responses and maturation of the MBC and BMPC responses, but we did not isolate any antibodies specifically targeting S proteins from the variant strains encoded by the mRNA-1273.213 vaccine that did not cross-react to the original WA1/2020 S protein. Thus, the B cell response after boosting with the mRNA-1273.213 vaccine was imprinted by the primary vaccination series with mRNA-1273, which encodes the ancestral S protein.

To determine whether a more antigenically divergent booster could generate a detectable response targeting novel epitopes, we recruited 8 participants who had received a 2-dose mRNA primary vaccination series and had no history of SARS-CoV-2 infection to receive 50 µg of mRNA-1273.529, which encodes BA.1 S protein (97.1% S protein and 93.3% RBD sequence conservation versus WA1/2020), as a first (third dose) or second (fourth dose at least 3 months after a third dose of mRNA-1273) booster (Extended Data Fig. 4a and Extended Data Tables 1 and 2). We analysed peripheral blood samples 1 and 17 weeks after the mRNA-1273.529 booster. All seven participants analysed one week after receiving the booster exhibited robust circulating IgG-producing plasmablast responses against the original WA1/2020 S protein as well as the vaccine-encoded BA.1 S protein, with lower IgA responses detectable in most participants (Fig. 3a and Extended Data Fig. 4b). To analyse the breadth of the MBC repertoire, we sorted MBCs from PBMCs isolated 17 weeks after the booster from participants 382-53, 382-54 and 382-55 (all of whom received mRNA-1273.529 as a third dose booster) using the same pooled fluorescent S protein probes from the WA1/2020, B.1.351, B.1.617.2 and BA.1 strains, to detect MBCs regardless of their strain specificity and to maintain consistency with the previously generated monoclonal antibodies. Similar to the monoclonal antibodies from the mRNA-1273 and mRNA-1273.213 cohorts, 303 out of 310 monoclonal antibodies (98%) were cross-reactive, binding S protein from WA1/2020, B.1.351 and B.1.617.2, including 220 (71%) that also recognized the BA.1 S protein encoded by the mRNA-1273.529 vaccine (Fig. 3b). Evaluation of the domains targeted by each monoclonal antibody revealed that 35% bound the RBD, 15% bound the NTD and 48% bound S2 (Fig. 3c). To assess the neutralization capacity of the MBC-derived monoclonal antibodies, we first screened all 730 S-binding monoclonal antibodies from the 3 cohorts with a high-throughput assay using chimeric vesicular stomatitis virus (VSV) in which the native envelope glycoprotein was replaced with S protein from the WA1/2020 strain with the D614G substitution<sup>32</sup>. Thirty monoclonal antibodies from the mRNA-1273 cohort, 49 from the mRNA-1273.213 cohort and 52 from the mRNA-1273.529 cohort neutralized infection by at least 80% at 5 µg ml<sup>-1</sup> (Extended Data Fig. 4c). We then evaluated the neutralizing capacity of these 131 monoclonal antibodies against a panel of authentic, infectious SARS-CoV-2 variants, including WA1/2020 D614G, B.1.351, B.1.617.2, BA.1 and BA.5, against which 67%, 47%, 67%, 10% and 10% from the mRNA-1273 cohort, 76%, 51%, 76%, 20% and 24% from the mRNA-1273.213 cohort, and 77%, 65%, 71%, 33% and 23% from the mRNA-1273.529 cohort, respectively, reduced infection by at least 90% at 5 µg ml<sup>-1</sup> (Fig. 3d).

Given the high frequency of cross-reactive monoclonal antibodies, we used a more targeted approach to sort MBCs specific for BA.1S protein that did not bind WA1/2020 S protein from participants 382-53, 382-54 and 382-55 (Fig. 4a). Sixty-five out of the seventy-eight monoclonal

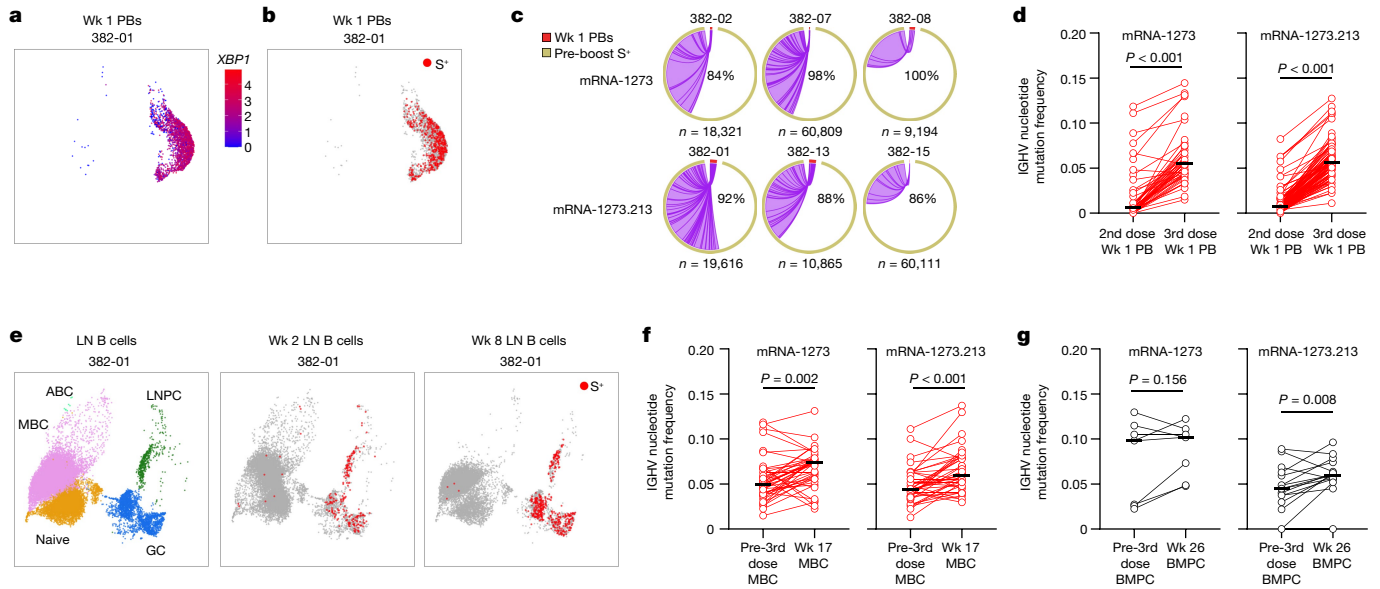


**Fig. 2 | Maturation of S protein-specific MBCs and BMPCs in response to mRNA-1273 or 1273.213 booster immunizations. a, b, e.** Uniform manifold approximation and projection (UMAP) of scRNA-seq transcriptional clusters of B cells from sorted circulating plasmablasts 1 week after booster immunization, with log-normalized *XBP1* gene expression (a) and S-specific clones (b) overlaid, or from FNAs of draining lymph nodes, with S-specific clones overlaid (e). Each dot represents a cell. **c.** Clonal overlap and percentages of S-specific plasmablast clones related to clones generated during the primary vaccine response among participants receiving mRNA-1273 (top) and mRNA-1273.213 (bottom). Peripheral arc lengths correspond to the number of B cell receptor sequences in the respective compartment and chord widths correspond to clone size. Purple chords connect clonally related sequences between plasmablast and

pre-boost arcs. Percentages are of plasmablast clones related to pre-boost S-specific clones. The number of sequences is indicated below each plot. **d, f, g.** Paired median IGHV gene mutation frequencies of S-specific clones found among plasmablasts 1 week after the second dose of the primary vaccine series and 1 week after booster vaccination (d), MBCs identified 6 months after primary vaccination and 17 weeks after booster vaccination (f), and BMPCs identified 6 and/or 9 months after primary vaccination and 6 months after booster vaccination (g). Each symbol represents the median mutation frequency of a clone; horizontal lines indicate medians. *P* values from two-sided Wilcoxon test. **d.** mRNA-1273, *n* = 52; mRNA-1273.213, *n* = 104. **f.** mRNA-1273, *n* = 42; mRNA-1273.213, *n* = 39. **g.** mRNA-1273, *n* = 7; mRNA-1273.213, *n* = 15.

antibodies (83%) isolated using this approach still cross-reacted with WA1/2020 S protein, indicating that the S-dependent sorting approach is not ideally sensitive for determining variant binding specificity. Out of the 78 monoclonal antibodies, 6 bound BA.1 S protein only, all of which were from participants 382-54 and 382-55 (Fig. 4b). Evaluation of the domains targeted by each monoclonal antibody revealed an increased proportion of NTD-targeting monoclonal antibodies at the expense of those specific for S2 compared with the monoclonal antibodies that were not sorted to exclude WA1/2020, with 31%, 53% and 10% binding RBD, NTD and S2, respectively (Fig. 4c). The SHM frequencies among the clonal families of the six monoclonal antibodies that bound BA.1 S protein but not WA1/2020 S protein were significantly

lower than those from the same participants that cross-reacted with WA1/2020 S protein (Fig. 4d). We tested the neutralizing capacity of the six monoclonal antibodies that bound BA.1 but not WA1/2020 against the panel of SARS-CoV-2 variants. As expected, none of the six antibodies neutralized the ancestral D614G strain. Notably, all six neutralized BA.1, one also neutralized BA.5 (17%) and none neutralized B.1.351 or B.1.617.2 at 5 μg ml<sup>-1</sup> (Fig. 4e). All six of the BA.1-neutralizing monoclonal antibodies targeted the RBD of S protein (Extended Data Fig. 4d). To identify the amino acid residues targeted by the six BA.1-specific monoclonal antibodies, we used VSV-SARS-CoV-2 chimeric viruses (S from BA.1 strain) to select variants that escaped neutralization, as previously described<sup>32,33</sup>. We performed plaque assays on Vero E6 cells

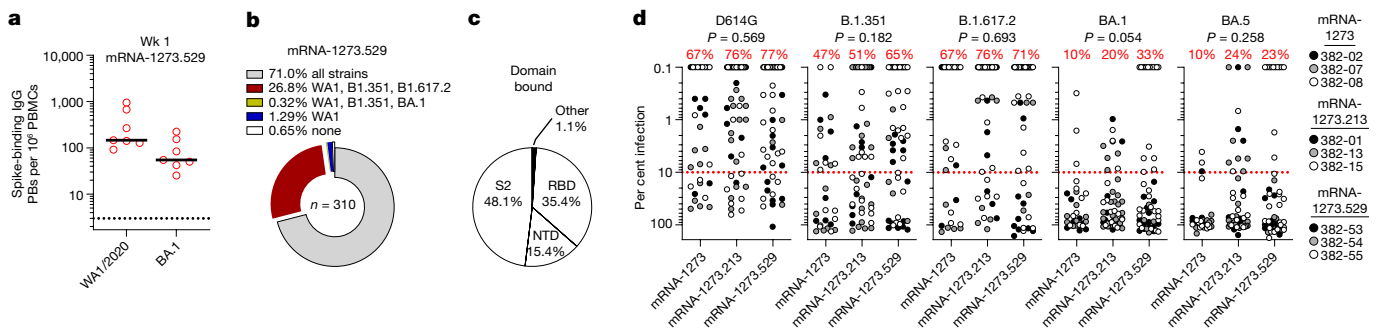


**Fig. 3 | Neutralization capacity of MBC-derived monoclonal antibodies. a.** Frequencies of S-binding IgG-producing plasmablasts in PBMC 1 week after booster vaccination, measured by ELISpot in participants who received mRNA-1273.529. Horizontal lines indicate medians. Each symbol represents a sample; *n* = 7. **b, c.** Binding of monoclonal antibodies from S<sup>+</sup> MBCs 17 weeks after mRNA-1273.529 booster immunization to S proteins from indicated SARS-CoV-2 strains (b) and constituent domains of WA1/2020 S protein (c),

measured by ELISA. **d.** Neutralizing activity of monoclonal antibodies from week 17 S<sup>+</sup> MBCs against indicated strains of authentic SARS-CoV-2 virus from participants who received indicated third-dose booster vaccines. Each symbol represents one monoclonal antibody. mRNA-1273, *n* = 30; mRNA-1273.213, *n* = 49; mRNA-1273.529, *n* = 52. Percentages indicate the proportion of monoclonal antibodies above the 90% infection reduction threshold. *P* values are from Chi-squared tests between the three vaccine cohorts.

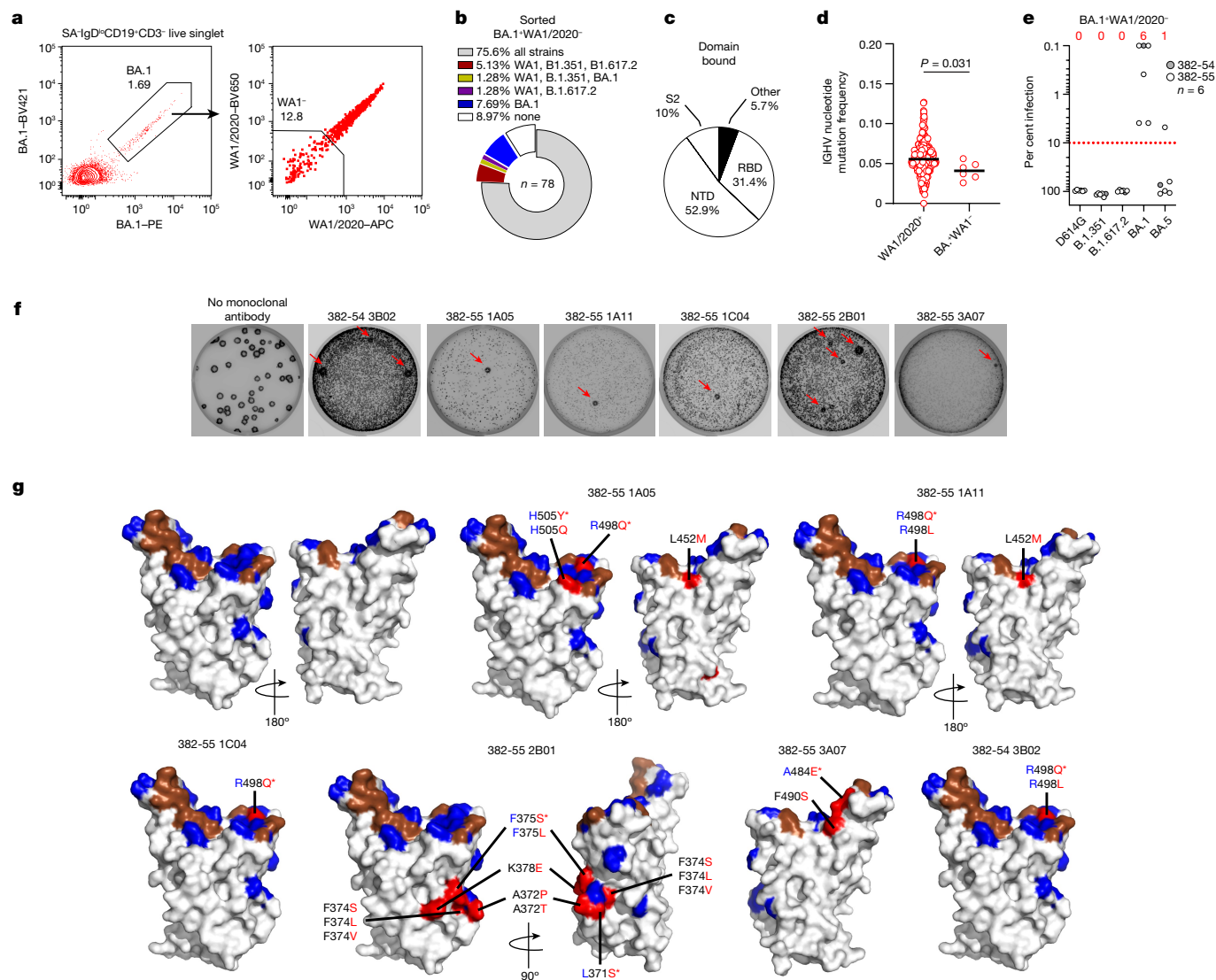


**Fig. 4 | Characterization of BA.1-specific monoclonal antibodies.** **a**, Gating strategy for sorting BA.1<sup>+</sup> WA1/2020<sup>-</sup> MBCs from PBMCs 17 weeks post booster. **b,c**, Binding of monoclonal antibodies from BA.1<sup>+</sup> WA1/2020<sup>-</sup> sorted MBCs to indicated strains of SARS-CoV-2 S protein (**b**), and constituent domains of S protein (**c**), measured by ELISA. **d**, IGHV mutation frequencies of clones related to monoclonal antibodies from participants 382-54 and 382-55 that bound WA1/2020 (left) and BA.1 but not WA1/2020 (right) S protein. Each symbol represents the median mutation frequency of a clone. WA1/2020<sup>+</sup>, *n* = 266; BA.1<sup>+</sup> WA1/2020<sup>-</sup>, *n* = 6. Black lines indicate medians. *P* value from two-sided Mann–Whitney test. **e**, Neutralizing activity of BA.1<sup>+</sup> WA1/2020<sup>-</sup> S-binding

monoclonal antibodies against indicated strains of authentic SARS-CoV-2 virus. Numbers above each virus are of monoclonal antibodies above the 90% infection reduction threshold. **f**, Plaque assays on Vero E6 cells with indicated monoclonal antibody in the overlay to isolate escape mutants (red arrows). Images are representative of three experiments per monoclonal antibody. **g**, Structure of the RBD with the human ACE2 footprint highlighted in brown. BA.1 mutations are highlighted in blue and amino acids whose substitution confers resistance to indicated monoclonal antibodies in plaque assays are highlighted in red. Asterisks indicate substitutions that confer resistance to the indicated monoclonal antibody and are reversions from BA.1 to the WA1/2020 sequence.

with the six neutralizing monoclonal antibodies in the overlay, purified the neutralization-resistant plaques, and sequenced the S genes (Fig. 4f and Extended Data Fig. 4e,f). Sequence analysis identified S protein escape mutations at R498 for monoclonal antibodies 382-54 3B02, 382-55 1A11 and 382-55 1C04; R498 and H505 for monoclonal antibody 382-55 1A05; L371, A372, F374, F375 and K378 for monoclonal antibody 382-55 2B01; and A484 and F490S for monoclonal antibody 382-55 3A07. Notably, many of the mutations were reversions to the ancestral strain of SARS-CoV-2. (Fig. 4g).

Here we have evaluated antigen-specific B cell responses to SARS-CoV-2 mRNA-based booster immunizations in humans. We show that boosting with ancestral SARS-CoV-2 or bivalent B.1.351/B.1.617.2-matched vaccines induce robust S-specific germinal centre responses in draining axillary lymph nodes of all sampled participants

that last until at least eight weeks after vaccination. S-specific plasmablasts and germinal centre B cells originate predominantly from pre-existing clonal lineages, consistent with most of the MBC-derived monoclonal antibodies that we isolated recognizing the original SARS-CoV-2 S protein. We also demonstrated that immunization with the monovalent B.1.1.529 BA.1-matched vaccine could induce rare de novo B cell responses against novel epitopes in the B.1.1.529 BA.1 S protein. These observations expand the large body of data showing improved potency and breadth of serum antibody responses after SARS-CoV-2 booster immunization in humans<sup>5–9,18</sup>.

Several critical insights relevant to cellular immunity to SARS-CoV-2 and recall responses to vaccination can be drawn from this study. B cell clones comprising the plasmablast compartment induced after the booster immunization were significantly more mutated than the

same clones detected one week after the completion of the primary vaccination series, a clear indication of the robust maturation process triggered by the primary vaccination<sup>2,29</sup>. Consistent with our previous work on B cell responses to seasonal influenza virus vaccination in humans<sup>34</sup>, the data presented here show that pre-existing MBCs can be efficiently re-engaged into recall germinal centre reactions. The frequencies of IgG-secreting BMPCs specific for the original SARS-CoV-2 S protein were several fold higher than those measured seven months after mild SARS-CoV-2 infections or six months after the primary mRNA vaccination series<sup>29,35</sup>. These increased frequencies are likely to be the result of the persistent germinal centre responses induced after the primary vaccination series and the new germinal centre reactions seeded by the booster immunization, highlighting the critical contribution of repeated antigen exposures to increasing antigen-specific BMPC frequency<sup>36,37</sup>.

A key unexpected finding in our study was the exceptionally high percentage of circulating MBCs that recognize the S protein from the original SARS-CoV-2 strain in the individuals boosted with variant S antigens, particularly as the booster immunizations did not encode S protein from the original strain. Of note, none of the participants from whom the monoclonal antibodies were derived had documented SARS-CoV-2 infection or seroconverted against the virus nucleocapsid protein during the course of the study. These data are consistent with MBCs generated by the primary vaccination series dominating the recall response induced by the booster and potentially out-competing clones specific for novel epitopes. It is possible that we were unable to isolate more memory B cell-derived monoclonal antibodies specific for novel epitopes on the B.1.351, B.1.617.2 or B.1.1.529 BA.1 S proteins because their affinity for the probes was below the limit of detection. The high antigenic similarity between the variant-derived and original SARS-CoV-2 S antigens in the case of the bivalent B.1.351/B.1.617.2 vaccine may have contributed to the low frequency of de novo clones recognizing the variants, and our data lend support for the decision to not adopt this vaccine for clinical use. Given the degree of cross-reactivity in the response we observed to purely variant-based vaccines, it is likely that the recently licensed bivalent boosters encoding WA1/2020 and either BA.1 or BA.4/5 will elicit similarly cross-reactive responses. We also speculate that an additional immunization with a variant-based vaccine may be needed to amplify the exclusively variant-specific B cell clones, similar to what has been observed upon H5N1 influenza virus immunization in humans<sup>38</sup>. We note that many of the mutations selected when we cultured recombinant vesicular stomatitis virus expressing SARS-CoV-2 Omicron (BA.1) S protein in the presence of the de novo monoclonal antibodies were reverted to the residues in the original strain. This suggests that newly escaped viruses are likely to be sensitive to potentially neutralizing antibodies, including some that were clinically approved for therapeutic use, that were thought to be no longer useful because of the changes at the E484 residue, for example<sup>39–43</sup>.

The high prevalence of MBCs recognizing the original SARS-CoV-2 S protein is evidence of antigenic imprinting, in which B cell responses to previously encountered antigens remain dominant even after exposure to different but antigenically related antigens<sup>44,45</sup>. Here we provide evidence that immunization with a distinct antigen can engage rare naive B cells that target novel epitopes, but the overall response remains dominated by clones that are cross-reactive to the original strain.

## Online content

Any methods, additional references, Nature Portfolio reporting summaries, source data, extended data, supplementary information, acknowledgements, peer review information; details of author contributions and competing interests; and statements of data and code availability are available at <https://doi.org/10.1038/s41586-023-06025-4>.

- Krause, P. R. et al. SARS-CoV-2 variants and vaccines. *N. Engl. J. Med.* **385**, 179–186 (2021).
- Turner, J. S. et al. SARS-CoV-2 mRNA vaccines induce persistent human germinal centre responses. *Nature* **596**, 109–113 (2021).
- Laidlaw, B. J. & Ellebedy, A. H. The germinal centre B cell response to SARS-CoV-2. *Nat. Rev. Immunol.* **22**, 7–18 (2022).
- Amanat, F. et al. SARS-CoV-2 mRNA vaccination induces functionally diverse antibodies to NTD, RBD, and S2. *Cell* **184**, 3936–3948.e10 (2021).
- Muecksch, F. et al. Increased memory B cell potency and breadth after a SARS-CoV-2 mRNA boost. *Nature* **607**, 128–134 (2022).
- Goel, R. R. et al. Efficient recall of Omicron-reactive B cell memory after a third dose of SARS-CoV-2 mRNA vaccine. *Cell* **185**, 1875–1887.e8 (2022).
- Rodda, L. B. et al. Imprinted SARS-CoV-2-specific memory lymphocytes define hybrid immunity. *Cell* **185**, 1588–1601.e14 (2022).
- Pérez-Then, E. et al. Neutralizing antibodies against the SARS-CoV-2 Delta and Omicron variants following heterologous CoronaVac plus BNT162b2 booster vaccination. *Nat. Med.* **28**, 481–485 (2022).
- Sette, A. & Crotty, S. Immunological memory to SARS-CoV-2 infection and COVID-19 vaccines. *Immunol. Rev.* **310**, 27–46 (2022).
- Lucas, C. et al. Impact of circulating SARS-CoV-2 variants on mRNA vaccine-induced immunity. *Nature* **600**, 523–529 (2021).
- Wang, Z. et al. mRNA vaccine-elicited antibodies to SARS-CoV-2 and circulating variants. *Nature* **592**, 616–622 (2021).
- Andrews, N. et al. Covid-19 vaccine effectiveness against the Omicron (B.1.1.529) variant. *N. Engl. J. Med.* **386**, 1532–1546 (2022).
- Kuhlmann, C. et al. Breakthrough infections with SARS-CoV-2 omicron despite mRNA vaccine booster dose. *Lancet* **399**, 625–626 (2022).
- Schmidt, F. et al. Plasma neutralization of the SARS-CoV-2 omicron variant. *N. Engl. J. Med.* **386**, 599–601 (2022).
- Cameroni, E. et al. Broadly neutralizing antibodies overcome SARS-CoV-2 Omicron antigenic shift. *Nature* **602**, 664–670 (2022).
- Cele, S. et al. Omicron extensively but incompletely escapes Pfizer BNT162b2 neutralization. *Nature* **602**, 654–656 (2022).
- Falsey, A. R. et al. SARS-CoV-2 Neutralization with BNT162b2 vaccine dose 3. *N. Engl. J. Med.* **385**, 1627–1629 (2021).
- Bowen, J. E. et al. Omicron spike function and neutralizing activity elicited by a comprehensive panel of vaccines. *Science* **377**, 890–894 (2022).
- Muik, A. et al. Neutralization of SARS-CoV-2 Omicron by BNT162b2 mRNA vaccine-elicited human sera. *Science* **375**, 678–680 (2022).
- Moreira, E. D. et al. Safety and efficacy of a third dose of BNT162b2 Covid-19 vaccine. *N. Engl. J. Med.* **386**, 1910–1921 (2022).
- Barda, N. et al. Effectiveness of a third dose of the BNT162b2 mRNA COVID-19 vaccine for preventing severe outcomes in Israel: an observational study. *Lancet* **398**, 2093–2100 (2021).
- Chalkias, S. et al. Safety, immunogenicity and antibody persistence of a bivalent Beta-containing booster vaccine against COVID-19: a phase 2/3 trial. *Nat. Med.* **28**, 2388–2397 (2022).
- Scheaffer, S. M. et al. Bivalent SARS-CoV-2 mRNA vaccines increase breadth of neutralization and protect against the BA.5 Omicron variant in mice. *Nat. Med.* **29**, 247–257 (2023).
- Jackson, L. A. et al. An mRNA vaccine against SARS-CoV-2—preliminary report. *N. Engl. J. Med.* **383**, 1920–1931 (2020).
- Walsh, E. E. et al. Safety and immunogenicity of two RNA-based Covid-19 vaccine candidates. *N. Engl. J. Med.* **383**, 2439–2450 (2020).
- Purtha, W. E., Tedder, T. F., Johnson, S., Bhattacharya, D. & Diamond, M. S. Memory B cells, but not long-lived plasma cells, possess antigen specificities for viral escape mutants. *J. Exp. Med.* **208**, 2599–2606 (2011).
- Lederer, K. et al. Germinal center responses to SARS-CoV-2 mRNA vaccines in healthy and immunocompromised individuals. *Cell* **185**, 1008–1024.e15 (2022).
- Röltgen, K. et al. Immune imprinting, breadth of variant recognition, and germinal center response in human SARS-CoV-2 infection and vaccination. *Cell* **185**, 1025–1040.e14 (2022).
- Kim, W. et al. Germinal centre-driven maturation of B cell response to mRNA vaccination. *Nature* **604**, 141–145 (2022).
- Gupta, N. T. et al. Hierarchical clustering can identify B cell clones with high confidence in Ig repertoire sequencing data. *J. Immunol.* **198**, 2489–2499 (2017).
- Zhou, J. Q. & Kleinstein, S. H. Cutting edge: Ig H chains are sufficient to determine most B cell clonal relationships. *J. Immunol.* **203**, 1687–1692 (2019).
- Case, J. B. et al. Neutralizing antibody and soluble ACE2 inhibition of a replication-competent VSV-SARS-CoV-2 and a clinical isolate of SARS-CoV-2. *Cell Host Microbe* **28**, 475–485.e5 (2020).
- Liu, Z. et al. Identification of SARS-CoV-2 spike mutations that attenuate monoclonal and serum antibody neutralization. *Cell Host Microbe* **29**, 477–488.e4 (2021).
- Turner, J. S. et al. Human germinal centres engage memory and naive B cells after influenza vaccination. *Nature* **586**, 127–132 (2020).
- Turner, J. S. et al. SARS-CoV-2 infection induces long-lived bone marrow plasma cells in humans. *Nature* **595**, 421–425 (2021).
- Radbruch, A. et al. Competence and competition: the challenge of becoming a long-lived plasma cell. *Nat. Rev. Immunol.* **6**, 741–750 (2006).
- Weisel, F. J., Zuccarino-Catania, G. V., Chikina, M. & Shlomchik, M. J. A temporal switch in the germinal center determines differential output of memory B and plasma cells. *Immunity* **44**, 116–130 (2016).
- Ellebedy, A. H. et al. Adjuvanted H5N1 influenza vaccine enhances both cross-reactive memory B cell and strain-specific naive B cell responses in humans. *Proc. Natl Acad. Sci. USA* **117**, 17957–17964 (2020).
- Zost, S. J. et al. Potently neutralizing and protective human antibodies against SARS-CoV-2. *Nature* **584**, 443–449 (2020).
- Chen, P. et al. SARS-CoV-2 neutralizing antibody LY-CoV555 in outpatients with COVID-19. *N. Engl. J. Med.* **384**, 229–237 (2021).

41. Hansen, J. et al. Studies in humanized mice and convalescent humans yield a SARS-CoV-2 antibody cocktail. *Science* **369**, 1010–1014 (2020).
42. Alsoussi, W. B. et al. A potently neutralizing antibody protects mice against SARS-CoV-2 infection. *J. Immunol.* **205**, 915–922 (2020).
43. Chen, R. E. et al. In vivo monoclonal antibody efficacy against SARS-CoV-2 variant strains. *Nature* **596**, 103–108 (2021).
44. Francis, T. On the doctrine of original antigenic sin. *Proc. Am. Philos. Soc.* **104**, 572–578 (1953).
45. Gostic, K. M., Ambrose, M., Worobey, M. & Lloyd-Smith, J. O. Potent protection against H5N1 and H7N9 influenza via childhood hemagglutinin imprinting. *Science* **354**, 722–726 (2016).

**Publisher's note** Springer Nature remains neutral with regard to jurisdictional claims in published maps and institutional affiliations.

Springer Nature or its licensor (e.g. a society or other partner) holds exclusive rights to this article under a publishing agreement with the author(s) or other rightsholder(s); author self-archiving of the accepted manuscript version of this article is solely governed by the terms of such publishing agreement and applicable law.

© The Author(s), under exclusive licence to Springer Nature Limited 2023

## Methods

### Sample collection, preparation and storage

All studies were approved by the Institutional Review Board of Washington University in St Louis. Written consent was obtained from all participants. Fifty-four healthy volunteers were enrolled, of whom 26 and 15 provided axillary lymph node and bone marrow aspirate samples, respectively (Extended Data Table 1). Blood samples were collected in ethylenediaminetetraacetic acid (EDTA) evacuated tubes (BD), and PBMCs were enriched by density gradient centrifugation over Lymphopure (BioLegend). The residual red blood cells were lysed with ammonium chloride lysis buffer, washed with PBS supplemented with 2% fetal bovine serum (FBS) and 2 mM EDTA (P2), and PBMC were immediately used or cryopreserved in 10% dimethylsulfoxide (DMSO) in FBS. Ultrasound-guided FNA of axillary lymph nodes was performed by a radiologist. Lymph node dimensions and cortical thickness were measured, and the presence and degree of cortical vascularity and location of the lymph node relative to the axillary vein were determined prior to each FNA. For each FNA sample, six passes were made under continuous real-time ultrasound guidance using 22- or 25-gauge needles, each of which was flushed with 3 ml of RPMI 1640 supplemented with 10% FBS and 100 U ml<sup>-1</sup> penicillin/streptomycin, followed by three 1-ml rinses. Red blood cells were lysed with ammonium chloride buffer (Lonza), washed with P2, and immediately used or cryopreserved in 10% DMSO in FBS. Participants reported no adverse effects from phlebotomies or serial FNAs. Bone marrow aspirates of approximately 30 ml were collected in EDTA tubes from the iliac crest. Bone marrow mononuclear cells were enriched by density gradient centrifugation over Ficoll-Paque PLUS (Cytiva), and remaining red blood cells were lysed with ammonium chloride buffer (Lonza) and washed with P2. BMPCs were enriched from bone marrow mononuclear cells using the EasySep Human CD138 Positive Selection Kit II (StemCell Technologies) and immediately used for ELISpot or cryopreserved in 10% DMSO in FBS.

### Cell lines

Expi293F cells were cultured in Expi293 Expression Medium (Gibco). Vero-TMPRSS2 cells<sup>46</sup> (a gift from S. Ding) were cultured at 37 °C in Dulbecco's modified Eagle medium (DMEM) supplemented with 10% FBS, 10 mM HEPES (pH 7.3), 1 mM sodium pyruvate, 1× nonessential amino acids, 100 U ml<sup>-1</sup> of penicillin/streptomycin, and 5 µg ml<sup>-1</sup> of blasticidin. Vero E6 cells were cultured at 37 °C in DMEM supplemented with 10% FBS, 10 mM HEPES (pH 7.3), 1 mM sodium pyruvate, 1× nonessential amino acids, and 100 U ml<sup>-1</sup> of penicillin/streptomycin.

### Antigens

Recombinant soluble S protein from WA1/2020, B.1.351, B.1.617.2 and B.1.1.529 (BA.1) strains of SARS-CoV-2 and their Avi-tagged counterparts were expressed as previously described<sup>29,47</sup>. In brief, mammalian cell codon-optimized nucleotide sequences coding for the soluble ectodomain of S (GenBank: MN908947.3, amino acids 1–1213) including a C-terminal thrombin cleavage site, T4 foldon trimerization domain, and hexahistidine tag were cloned into mammalian expression vector pCAGGS. The S sequences were modified to remove the polybasic cleavage site (RRAR to A), and two prefusion stabilizing proline mutations were introduced (K986P and V987P, wild type numbering). For expression of Avi-tagged variants, the CDS of pCAGGS vector containing the sequence for the relevant soluble S was modified to encode 3' Avitag insert after the 6×His tag (5'-His tag-GGCTCCGGGCTGACGACATCTTCGAAGCCCAGAAGATTGAGTGGCATGAG-Stop-3'; HHH HHHGSLNDIFEAQKIEWHE-) using inverse PCR mutagenesis as previously described<sup>48</sup>. Recombinant proteins were produced in Expi293F cells (ThermoFisher) by transfection with purified DNA using the ExpiFectamine 293 Transfection Kit (ThermoFisher). Supernatants from transfected cells were collected 3 days post-transfection, and recombinant proteins were purified using Ni-NTA agarose (ThermoFisher), then

buffer exchanged into PBS and concentrated using Amicon Ultracel centrifugal filters (EMD Millipore). To biotinylate Avi-tagged S variants, the S-Avitag substrates were diluted to 40 µM and incubated for 1 h at 30 °C with 15 µg ml<sup>-1</sup> BirA enzyme (Avidity) in 0.05 M bicine buffer at pH 8.3 supplemented with 10 mM ATP, 10 mM magnesium acetate and 50 µM biotin. The protein was then concentrated and buffer exchanged with PBS using a 100 kDa Amicon Ultra centrifugal filter (EMD Millipore).

To generate antigen probes for flow cytometry staining and sorting, trimeric BirA-biotinylated recombinant S from WA1/2020, B.1.351, B.1.617.2, or B.1.1.529 (BA.1) were incubated with a 1.04-fold molar excess of BV421-, BV650-, or PE-conjugated streptavidin (BioLegend), on ice, with three equal additions of S spaced every 15 min. Fifteen minutes after the third S addition, d-biotin was added in sixfold molar excess to streptavidin to block any unoccupied biotin binding sites. Streptavidin-PE-Cy5 and streptavidin-APC-Fire750 (BioLegend) were blocked with a 6-fold molar excess of d-biotin and used as background staining controls. Bovine serum albumin (BSA) was biotinylated using the EZ-Link Micro NHS-PEG4-Biotinylation Kit (Thermo Fisher); excess unreacted biotin was removed using 7-kDa Zeba desalting columns (Pierce).

### ELISpot assay

Wells were coated with Flucelvac Quadrivalent 2019/2020 seasonal influenza virus vaccine (Sequiris), recombinant S from the WA1/2020, B.1.351, B.1.617.2, or BA.1 strains of SARS-CoV-2, or pooled anti-κ and anti-λ light chain antibodies (Cellular Technology Limited). Direct ex vivo ELISpot assays were performed with non-cryopreserved PBMCs to determine the number of total, influenza vaccine-binding, or recombinant S-binding IgG- and IgA-secreting cells present in PBMC and non-cryopreserved enriched BMPC samples using IgG/IgA double-colour ELISpot Kits (Cellular Technology Limited) according to the manufacturer's instructions. ELISpot plates were analysed using an ELISpot counter (Cellular Technology Limited).

### Fluorescent bead antigen binding assay

Recombinant biotinylated S from WA1/2020, B.1.351, B.1.617.2 and BA.1 strains of SARS-CoV-2 and biotinylated BSA were incubated for 30 min on ice with different fluorescence intensity peaks of the Streptavidin Coated Fluorescent Yellow Particle Kit (Spherotech) at 9.12 ng per µg beads. Beads were washed twice with 0.05% Tween 20 in PBS, resuspended in monoclonal antibodies diluted to 65 µg ml<sup>-1</sup> or plasma samples diluted 1:80 in 0.05% Tween 20 in PBS, and incubated for 30 min on ice. Beads were washed twice with 0.05% Tween 20 in PBS, stained with IgG-APC-Fire750 (M1310G05, BioLegend, 1:100), incubated for 30 min on ice, washed twice with 0.05% Tween 20 in PBS, and resuspended in 2% FBS and 2 mM EDTA in PBS and acquired on an Aurora using SpectroFlo v2.2 (Cytel). Data were analysed using FlowJo v10 (Treestar). Background-subtracted median fluorescence intensities were calculated for each sample by subtracting its median fluorescence intensity plus two times robust standard deviation for BSA and the median fluorescence intensity of an influenza virus haemagglutinin-specific monoclonal antibody (for monoclonal antibody samples) or plasma collected prior to the SARS-CoV-2 pandemic (for plasma samples) for the respective spike variant (Extended Data Fig. 1b).

### ELISA

Assays were performed in 96-well plates (MaxiSorp; Thermo) coated with 100 µl of recombinant S from WA1/2020, B.1.351, B.1.617.2 and BA.1 strains of SARS-CoV-2, NTD of WA1/2020 or BA.1, receptor binding domain of WA1/2020 or BA.1, or S2 domain of WA1/2020, or bovine serum albumin diluted to 1 µg ml<sup>-1</sup> in PBS, and plates were incubated at 4 °C overnight. Plates then were blocked with 10% FBS and 0.05% Tween 20 in PBS. Purified monoclonal antibodies were serially diluted in blocking buffer and added to the plates. Plates were incubated for 90 min at room temperature and then washed 3 times with 0.05% Tween



# Article

20 in PBS. Goat anti-human IgG-HRP (goat polyclonal, Jackson ImmunoResearch, 1:2,500) was diluted in blocking buffer before adding to plates and incubating for 60 min at room temperature. Plates were washed 3 times with 0.05% Tween 20 in PBS and 3 times with PBS before the addition of *O*-phenylenediamine dihydrochloride peroxidase substrate (Sigma-Aldrich). Reactions were stopped by the addition of 1 M hydrochloric acid. Optical density measurements were taken at 490 nm.

## VSV-SARS-CoV-2-S<sub>Δ21</sub> eGFP-reduction assay

The S gene of SARS-CoV-2 isolate WA1/2020 (with D614G mutation) was synthesized and replaced the native envelope glycoprotein of an infectious molecular clone of VSV, and resulting chimeric viruses expressing S protein from SARS-CoV-2 D614G were used for GFP reduction neutralization tests as previously described<sup>32</sup>. In brief, 10<sup>3</sup> PFU of VSV-SARS-CoV-2-S<sub>Δ21</sub> was incubated for 1 h at 37 °C with recombinant monoclonal antibodies diluted to 5 μg ml<sup>-1</sup>. Antibody-virus complexes were added to Vero E6 cells in 96-well plates and incubated at 37 °C for 7.5 h. Cells were subsequently fixed in 2% formaldehyde (Electron Microscopy Sciences) containing 10 μg ml<sup>-1</sup> Hoechst 33342 nuclear stain (Invitrogen) for 45 min at room temperature, when fixative was replaced with PBS. Images were acquired with an InCell 2000 Analyzer (GE Healthcare) automated microscope using the DAPI and FITC channels to visualize nuclei and infected cells (that is, eGFP-positive cells), respectively (4× objective, 4 fields per well, covering the entire well). Images were analysed using the Multi Target Analysis Module of the InCell Analyzer 1000 Workstation Software (GE Healthcare). GFP-positive cells were identified in the FITC channel using the top-hat segmentation method and subsequently counted within the InCell Workstation software. The sensitivity and accuracy of GFP-positive cell number determinations were validated using a serial dilution of virus. The percent infection reduction was calculated from wells to which no antibody was added. A background number of GFP-positive cells was subtracted from each well using an average value determined from at least four uninfected wells.

## Focus reduction neutralization test

Each monoclonal antibody was incubated at 5 μg ml<sup>-1</sup> in DMEM supplemented with 2% FBS, 10 mM HEPES, and 100 U ml<sup>-1</sup> penicillin/streptomycin with 10<sup>2</sup> focus-forming units of different SARS-CoV-2 strains (WA1/2020 D614G, B.1.351, B.1.617.2, BA.1, and BA.5) for 1 h at 37 °C<sup>49</sup>. Antibody-virus complexes were added to Vero-TMPRSS2 cell monolayers in 96-well plates and incubated at 37 °C for 1 h. Subsequently, cells were overlaid with 1% (w/v) methylcellulose in MEM supplemented with 2% FBS. Plates were harvested 30 h (D614G, B.1.351, or B.1.617.2-infected) or 70 h (BA.1 or BA.5-infected) later by removing overlays and fixed with 4% PFA in PBS for 20 min at room temperature. Plates were washed and incubated with an oligoclonal pool of anti-S antibodies (SARS2-2, SARS2-11, SARS2-16, SARS2-31, SARS2-38, SARS2-57, and SARS2-71)<sup>33</sup>, and an additional oligoclonal pool of anti-S antibodies with extended reactivity (SARS2-08, SARS2-09, SARS2-10, SARS2-13, SARS2-14, SARS2-17, SARS2-20, SARS2-26, SARS2-27, SARS2-28, SARS2-31, SARS2-41, SARS2-42, SARS2-44, SARS2-49, SARS2-62, SARS2-64, SARS2-65 and SARS2-67)<sup>50</sup> were included for staining BA.1- or BA.5-infected plates. Plates were subsequently incubated with HRP-conjugated goat anti-mouse IgG (Sigma 12-349) in PBS supplemented with 0.1% saponin and 0.1% bovine serum albumin. SARS-CoV-2-infected cell foci were visualized using TrueBlue peroxidase substrate (KPL) and quantitated on an ImmunoSpot microanalyzer (Cellular Technologies Limited).

## Selection of monoclonal antibody escape mutants in SARS-CoV-2 S

We generated VSV-SARS-CoV-2-S (BA.1 variant) chimera by inserting the BA.1 spike gene into the VSV genome and using the resulting VSV-SARS-CoV-2 BA.1 chimeric virus to select for SARS-CoV-2 S variants that escape monoclonal antibody neutralization as described previously<sup>32,33</sup>.

Antibody neutralization-resistant mutants were recovered by plaque isolation. In brief, plaque assays were performed to isolate the VSV-SARS-CoV-2 escape mutant on Vero cells with each tested monoclonal antibody in the overlay. The concentration of each monoclonal antibody in the overlay was determined by neutralization assays at a multiplicity of infection of 100. Escape clones were plaque-purified on Vero cells in the presence of monoclonal antibodies, and plaques in agarose plugs were amplified on MA104 cells with the monoclonal antibodies present in the medium. Viral supernatants were collected after three days upon extensive cytopathic effect and clarified of cell debris by centrifugation at 1,000g for 5 min. Aliquots were maintained at -80 °C. Viral RNA was extracted from VSV-SARS-CoV-2 mutant viruses using RNeasy Mini kit (Qiagen), and the S gene was amplified using OneStep RT-PCR Kit (Qiagen). To sequence the 3,747-bp BA.1 spike gene, four sets of PCR were set up to efficiently cover the whole BA.1 spike gene in the virus as follows: first set of fragment PCR utilizing sequencing primers 15M (ctggattctatcagccac) and 369 (caatagattctgttggttg); second set of fragment PCR utilizing sequencing primers 368 (ctctctcagaacaa gtgt) and 372 (cctgcacgtgttgaaaa); third set of fragment PCR utilizing sequencing primers 370 (aactgcacagaagtcct) and 374 (agaacattctgtg taactc); and fourth set of fragment PCR utilizing sequencing primers 373 (tacaatcactctgtgttga) and 23L (cattgaactctgctgtctc) (Extended Data Fig. 4f). The mutations were identified by Sanger sequencing (Genewiz).

## Cell sorting and flow cytometry

Staining for flow cytometry analysis and sorting was performed using freshly isolated or cryopreserved FNA or PBMC samples. For analysis, PBMC were incubated for 30 min on ice with purified CD16 (3G8, BioLegend, 1:100), CD32 (FUN-2, BioLegend, 1:100), CD64 (10.1, BioLegend, 1:100) and PD-1-BB515 (EH12.1, BD Horizon, 1:100) in 2% FBS and 2 mM EDTA in PBS (P2), washed twice, then were stained for 30 min on ice with WA1/2020, B.1.351, B.1.617.2 and BA.1 spike probes pre-conjugated to SA-BV650 and SA-PE, S<sub>167-180</sub>-PE-Cy7 tetramer, S<sub>816-830</sub>-APC tetramer<sup>51</sup>, biotin-saturated SA-PE-Cy5, ICOS-SB436 (ISA-3, Invitrogen, 1:50), IgG-BV480 (goat polyclonal, Jackson ImmunoResearch, 1:100), IgA-FITC (M24A, Millipore, 1:500), CD8a-A532 (RPA-T8, Thermo, 1:100), CD38-BB700 (HIT2, BD Horizon, 1:500), CD71-BV421 (CY1G4, 1:400), CD20-Pacific Blue (2H7, 1:400), CD4-Spark Violet 538 (SK3, 1:400), CD19-BV750 (HIB19, 1:100), IgD-BV785 (IA6-2, 1:200), CXCR5-PE-Dazzle 594 (J252D4, 1:50), CD14-PerCP (HCD14, 1:50), CD27-PE-Fire810 (O323, 1:200), CCR7-Spark 685 (G043H7, 1:100), IgM-A700 (MHM-88, 1:400), CD3-APC-Fire810 (SK7, 1:50), and Zombie NIR (all BioLegend) diluted in Brilliant Staining buffer (BD Horizon). For analysis, FNA samples were incubated for 30 min on ice with purified CD16 (3G8, BioLegend, 1:100), CD32 (FUN-2, BioLegend, 1:100), CD64 (10.1, BioLegend, 1:100) and PD-1-BB515 (EH12.1, BD Horizon, 1:100) in P2, washed twice, then stained for 30 min on ice with WA1/2020, B.1.351, B.1.617.2, and B.1.1.529 spike probes pre-conjugated to SA-BV421 and SA-BV650, S<sub>167-180</sub>-APC tetramer, biotin-saturated SA-PE-Cy5, IgG-BV480 (goat polyclonal, Jackson ImmunoResearch, 1:100), IgA-FITC (M24A, Millipore, 1:500), CD8a-A532 (RPA-T8, Thermo, 1:100), CD38-BB700 (HIT2, BD Horizon, 1:500), CD20-Pacific Blue (2H7, 1:400), CD4-Spark Violet 538 (SK3, 1:400), IgM-BV605 (MHM-88, 1:100), CD19-BV750 (HIB19, 1:100), IgD-BV785 (IA6-2, 1:200), CXCR5-PE-Dazzle 594 (J252D4, 1:50), CD14-PerCP (HCD14, 1:50), CD71-PE-Cy7 (CY1G4, 1:400), CD27-PE-Fire810 (O323, 1:200), CD3-APC-Fire810 (SK7, 1:50) and Zombie NIR (all BioLegend) diluted in Brilliant Staining buffer (BD Horizon). Cells were washed twice with P2, fixed for 1 h at 25 °C using the True Nuclear fixation kit (BioLegend), washed twice with True Nuclear Permeabilization/Wash buffer, stained with Ki-67-BV711 (Ki-67, BioLegend, 1:200), Blimp1-PE (646702, R&D, 1:100), FOXP3-Spark 685 (206D, BioLegend, 1:200), and Bcl6-R718 (K112-91, BD Horizon, 1:200) for 1 h at 25 °C, and washed twice with True Nuclear Permeabilization/Wash buffer. Samples were resuspended in P2 and

acquired on an Aurora using SpectroFlo v2.2 (Cytex). Flow cytometry data were analysed using FlowJo v10 (Treestar).

For sorting plasmablasts, PBMCs collected 1 week post-boost were stained for 30 min on ice with CD20–Pacific Blue (2H7, 1:400), CD71–FITC (CY1G4, 1:200), IgD–PerCP–Cy5.5 (IA6-2, 1:200), CD19–PE (HIB19, 1:200), CXCR5–PE–Dazzle 594 (J252D4, 1:50), CD38–PE–Cy7 (HIT2, 1:200), CD4–A700 (SK3, 1:400) and Zombie Aqua (all BioLegend) diluted in P2. Cells were washed twice, and plasmablasts (live singlet CD4<sup>+</sup>CD19<sup>+</sup>IgD<sup>lo</sup>CD20<sup>lo</sup>CD38<sup>+</sup>CXCR5<sup>lo</sup>CD71<sup>+</sup>) were sorted using a Bigfoot (Invitrogen) into PBS supplemented with 0.05% BSA and immediately processed for scRNA-seq. For bulk sorting germinal centre and LNPC, lymph node FNA samples collected 2 or 8 weeks post-boost were stained for 30 min on ice with purified CD16 (3G8, BioLegend, 1:100), CD32 (FUN-2, BioLegend, 1:100), CD64 (10.1, BioLegend, 1:100) and PD-1–BB515 (EH12.1, BD Horizon, 1:100) in P2, washed twice, then stained for 30 min on ice with CD20–Pacific Blue (2H7, 1:400), CD19–BV750 (HIB19, 1:100), IgD–PerCP–Cy5.5 (IA6-2, 1:200), CD71–PE (CY1G4, 1:400), CXCR5–PE–Dazzle 594 (J252D4, 1:50), CD38–PE–Cy7 (HIT2, 1:200), CD4–A700 (SK3, 1:400) and Zombie Aqua (all BioLegend) diluted in P2. Cells were washed twice, and total germinal centre B cells (live singlet CD4<sup>+</sup>CD19<sup>+</sup>IgD<sup>lo</sup>CD20<sup>+</sup>CD38<sup>int</sup>CXCR5<sup>+</sup>CD71<sup>+</sup>) and LNPC (live singlet CD4<sup>+</sup>CD19<sup>+</sup>IgD<sup>lo</sup>CD20<sup>lo</sup>CD38<sup>+</sup>CXCR5<sup>lo</sup>CD71<sup>+</sup>) were sorted using a Bigfoot (Invitrogen) into Buffer RLT Plus (Qiagen) supplemented with 143 mM  $\beta$ -mercaptoethanol (Sigma-Aldrich) and immediately frozen on dry ice. For sorting memory B cells, PBMC collected 17 weeks post-boost were incubated for 10 min on ice with purified CD16 (3G8, BioLegend, 1:100), CD32 (FUN-2, BioLegend, 1:100), and CD64 (10.1, BioLegend, 1:100) in P2. For sorting S<sup>+</sup> memory B cells, WA1/2020, B.1.351, B.1.617.2 and BA.1 spike probes pre-conjugated to SA–BV650 and SA–PE, biotin-saturated SA–PE–Cy5, CD20–Pacific Blue (2H7, 1:400), CD19–BV605 (HIB19, 1:100), IgD–BV785 (IA6-2, 1:200), CD3–FITC (HIT3a, 1:200), CD27–A700 (M-T271, 1:200) and Zombie NIR (all BioLegend) diluted in Brilliant Staining buffer (BD Horizon) were added and stained for an additional 30 min on ice. For sorting BA.1<sup>+</sup> WA1/2020<sup>+</sup> memory B cells, WA1/2020 probes pre-conjugated to SA–BV650 and SA–APC, BA.1 probes pre-conjugated to SA–BV421 and SA–PE, biotin-saturated SA–PE–Cy5, CD20–Pacific Blue (2H7, 1:400), IgD–BV785 (IA6-2, 1:200), CD19–FITC (HIB19, 1:100), CD27–PE–Fire810 (O323, 1:200), CD3–A700 (HIT3a, 1:100) and Zombie NIR (all BioLegend) diluted in Brilliant Staining buffer (BD Horizon) were added and stained for an additional 30 min on ice. Cells were washed twice, and pooled S-binding single memory B cells (live singlet CD3<sup>+</sup>CD19<sup>+</sup>IgD<sup>lo</sup>SA–PE–Cy5<sup>+</sup> pooled spikes double positive) or BA.1<sup>+</sup> WA1/2020<sup>+</sup> single memory B cells (live singlet CD3<sup>+</sup>CD19<sup>+</sup>IgD<sup>lo</sup>SA–PE–Cy5<sup>+</sup> BA.1<sup>+</sup> WA1/2020<sup>+</sup>) were sorted using a Bigfoot (Invitrogen) into 96-well plates containing 2  $\mu$ l Lysis Buffer (Clontech) supplemented with 1 U  $\mu$ l<sup>-1</sup> RNase inhibitor (NEB), or total IgD<sup>lo</sup> memory B cells were bulk sorted into Buffer RLT Plus (Qiagen) supplemented with 143 mM  $\beta$ -mercaptoethanol (Sigma-Aldrich) and immediately frozen on dry ice.

### Monoclonal antibody generation

Antibodies were cloned as described previously<sup>52</sup>. In brief, VH, Vk and VL genes were amplified by PCR with reverse transcription and nested PCR reactions from singly-sorted S<sup>+</sup> memory B cells using primer combinations specific for IgG, IgM/A, Igk and Igl from previously described primer sets<sup>53</sup> and then sequenced. To generate recombinant antibodies, restriction sites were incorporated via PCR with primers to the corresponding heavy and light chain V and J genes. The amplified VH, Vk and VL genes were cloned into IgG1 and Igk or Igl expression vectors, respectively, as described previously<sup>53–55</sup>. Heavy and light chain plasmids were co-transfected into Expi293F cells (Gibco) for expression, and antibody was purified using protein A agarose chromatography (Goldbio). Sequences were obtained from PCR reaction products and annotated using the ImMunoGeneTics (IMGT)/V-QUEST database ([http://www.imgt.org/IMGT\\_vquest/](http://www.imgt.org/IMGT_vquest/))<sup>56,57</sup>. Mutation frequency was

calculated by counting the number of nonsynonymous nucleotide mismatches from the germline sequence in the heavy chain variable segment leading up to the CDR3, while excluding the 5' primer sequences that could be error-prone.

### scRNA-seq library preparation and sequencing

Sorted plasmablast and lymph node FNA samples were processed using the following 10x Genomics kits: Chromium Next GEM Single Cell 5' Kit v2 (PN-1000263); Chromium Next GEM Chip K Single Cell Kit (PN-1000286); BCR Amplification Kit (PN-1000253); Dual Index Kit TT Set A (PN-1000215). Chromium Single Cell 5' Gene Expression Dual Index libraries and Chromium Single Cell V(D)J Dual Index libraries were prepared according to manufacturer's instructions. Both gene expression and V(D)J libraries were sequenced on a Novaseq S4 (Illumina), targeting a median sequencing depth of 50,000 and 5,000 read pairs per cell, respectively.

### Bulk BCR library preparation and sequencing

RNA was purified from sorted plasmablasts and memory B cells from PBMC, germinal centre B cells and plasma cells from lymph node FNA (LNPC), and CD138-enriched BMPC using the RNeasy Plus Micro kit (Qiagen). Reverse transcription, unique molecular identifier (UMI) barcoding, cDNA amplification, and Illumina linker addition to B cell heavy chain transcripts were performed using the human NEBNext Immune Sequencing Kit (New England Biolabs) according to the manufacturer's instructions. High-throughput 2 $\times$  300 bp paired-end sequencing was performed on the Illumina MiSeq platform with a 30% PhiX spike-in according to manufacturer's recommendations, except for performing 325 cycles for read 1 and 275 cycles for read 2.

### Preprocessing of bulk sequencing BCR reads

Preprocessing of demultiplexed pair-end reads was performed using pRESTO v.0.6.2<sup>58</sup> as previously described<sup>2</sup>, with the exception that sequencing errors were corrected using the UMIs as they were without additional clustering (Extended Data Table 3). Previously preprocessed unique consensus sequences from samples corresponding to participants in the current study and previously reported in ref. 29 were included without additional processing. Participants 382-01, 382-02, 382-07, 382-08, 382-13, and 382-15 correspond to previously reported 368-22, 368-20, 368-02a, 368-04, 368-01a and 368-10, respectively<sup>2,29</sup>. Previously preprocessed unique consensus sequences from samples corresponding to participants in the current study and reported in<sup>2</sup> were subset to those with at least two contributing reads and included.

### Preprocessing of 10x Genomics single-cell BCR reads

Demultiplexed pair-end FASTQ reads were preprocessed using Cell Ranger v.6.0.1 as previously described<sup>29</sup> (Extended Data Table 4). Previously preprocessed single-cell BCR reads from samples corresponding to participants in the current study and reported in ref. 29 were included.

### V(D)J gene annotation and genotyping

Initial germline V(D)J gene annotation was performed on the preprocessed BCRs using IgBLAST v.1.17.1<sup>59</sup> with the deduplicated version of IMGT/V-QUEST reference directory release 202113-2<sup>56</sup>. Further sequence-level and cell-level quality controls were performed as previously described<sup>29</sup>. Exceptions for monoclonal antibody sequences triggering QC filters were handled on a case-by-case basis upon inspection as follows. Indels detected in 382-01 1B04 heavy chain and 1F01 light chain and 382-53 2G07 heavy chain were accepted. The CDR3 annotations from IMGT/V-QUEST for 382-08 1G04 heavy chain, 382-54 1D09 heavy chain and 382-55 4H10 light chain were used in lieu of those from IgBLAST as the former had nucleotide lengths that were a multiple of 3 whereas the latter did not. Individualized genotypes were inferred based on sequences that passed all quality controls using

# Article

TigGER v.1.0.0<sup>60</sup> and used to finalize V(D)J annotations. Sequences annotated as non-productively rearranged by IgBLAST were removed from further analysis.

## Clonal lineage inference

B cell clonal lineages were inferred on a by-individual basis based on productively rearranged sequences as previously described<sup>29</sup>. In brief, heavy chain-based clonal inference<sup>31</sup> was performed by partitioning the heavy chains of bulk and single-cell BCRs based on common V and J gene annotations and CDR3 lengths, and clustering the sequences within each partition hierarchically with single linkage based on their CDR3s<sup>30</sup>. Sequences whose CDR3 nucleotides were within 0.15 normalized Hamming distance from each other were clustered as clones. Following clonal inference, full-length clonal consensus germline sequences were reconstructed using Change-O v.1.0.2<sup>61</sup>. Within each clone, duplicate IMGT-aligned V(D)J sequences from bulk sequencing were collapsed using Alakazam v.1.0.0<sup>61</sup> except for duplicates derived from different lymph nodes, time points, tissues, B cell compartments, isotypes, or biological replicates.

## BCR analysis

B cell compartment labels were treated as previously described<sup>29</sup>. In brief, gene expression-based cluster annotation was used for single-cell BCRs; FACS-based sorting and magnetic enrichment were used for bulk BCRs, except that plasmablast sorts from lymph node FNA were labelled LNPCs; post-second dose week 2 IgD<sup>lo</sup> enriched B cells from blood were labelled activated; and post-second dose week 4 and post-third dose (booster) week 17 IgD<sup>lo</sup> enriched B cells from blood were labelled memory. For analysis involving the memory compartment, the memory sequences were restricted to those from blood. A heavy chain-based B cell clone was considered S-specific if it contained any sequence corresponding to a S-binding monoclonal antibody that was previously reported<sup>2,29</sup> or from the current study. Clonal overlap between B cell compartments was visualized using circize v.0.4.13<sup>62</sup>. SHM frequency was calculated for each heavy chain sequence using SHazaM v.1.0.2<sup>61</sup> as previously described<sup>29</sup> by counting the number of nucleotide mismatches from the germline sequence in the variable segment leading up to the CDR3, while excluding the first 18 positions that could be error-prone due to the primers used for generating the monoclonal antibody sequences.

## Processing of 10x Genomics single-cell 5' gene expression data

Demultiplexed pair-end FASTQ reads were first preprocessed on a by-sample basis and samples were subsequently subsampled to the same effective sequencing length and aggregated using Cell Ranger v.6.0.1 as previously described<sup>29</sup>. Quality control was performed on the aggregate gene expression matrix consisting of 336,960 cells and 36,601 features using SCANPY v.1.7.2<sup>63</sup>. In brief, to remove presumably lysed cells, cells with mitochondrial content greater than 17.5% of all transcripts were removed. To remove likely doublets, cells with more than 8,000 features or 80,000 total UMIs were removed. To remove cells with no detectable expression of common endogenous genes, cells with no transcript for any of a list of 34 housekeeping genes<sup>29</sup> were removed. The feature matrix was subset, based on their biotypes, to protein-coding, immunoglobulin, and T cell receptor genes that were expressed in at least 0.05% of the cells in any sample. The resultant feature matrix contained 15,751 genes. Finally, cells with detectable expression of fewer than 200 genes were removed. After quality control, there were a total of 312,242 cells from 39 single-cell samples (Extended Data Table 4).

## Single-cell gene expression analysis

Transcriptomic data was analysed using SCANPY v.1.7.2<sup>63</sup> as previously described<sup>29</sup> with minor adjustments suitable for the current data. In brief, overall clusters were first identified using Leiden graph-clustering with

resolution 0.50 (Extended Data Fig. 3b, Extended Data Table 5). UMAPs were faceted by participant and inspected for convergence to assess whether there was a need for integration (Extended Data Fig. 3c). Cluster identities were assigned by examining the expression of a set of marker genes<sup>34</sup> for different cell types (Extended Data Fig. 3d). To remove potential contamination by platelets, 205 cells with a log-normalized expression value of >2.5 for PPBP were removed. From a cluster consisting primarily of monocytes, 36 cells originating from lymph node FNA and with a log-normalized expression value of >0 for at least two of FDCSP, CXCL14<sup>64</sup>, and FCAMR<sup>65</sup> were annotated FDCs. Cells from the overall B cell cluster were further clustered to identify B cell subsets using Leiden graph-clustering resolution 0.35 (Extended Data Fig. 3e and Extended Data Table 5). Cluster identities were assigned by examining the expression of a set of marker genes<sup>34</sup> for different B cell subsets (Extended Data Fig. 3f) along with the availability of BCRs. Despite being clustered with B cells during overall clustering, one group tended to have both BCRs and relatively high expression levels of CD2 and CD3E; one group tended to have no BCRs and relatively high CD2 and CD3E; and two unassigned groups tended to have no BCRs. These were excluded from the final B cell clustering. Ten cells that were found in the germinal centre B cell cluster but came from blood were labelled 'PB-like'<sup>34</sup>. Four-hundred and seven cells that were found in the PB cluster but came from lymph node FNA were re-assigned as LNPCs. One cell that was found in the LNPC cluster but came from blood was re-assigned as PB. Heavy chain SHM frequency and isotype usage of the B cell subsets were inspected for consistency with expected values to further confirm their assigned identities.

## Reporting summary

Further information on research design is available in the Nature Portfolio Reporting Summary linked to this article.

## Data availability

Antibody sequences have been deposited in GenBank under accession numbers OQ634308–OQ635939. Newly reported raw sequencing data and the transcriptomics count matrix are deposited at the Sequence Read Archive and Gene Expression Omnibus under BioProject PRJNA800176. Processed transcriptomics and BCR data are deposited at Zenodo (<https://doi.org/10.5281/zenodo.7719030>). Previously reported BCR data used in this study were deposited under BioProjects PRJNA731610, PRJNA741267 and PRJNA777934. The IMGT/V-QUEST database is accessible at [http://www.imgt.org/IMGT\\_vquest/](http://www.imgt.org/IMGT_vquest/). Materials are available upon request through an interinstitutional materials transfer agreement.

- Zang, R. et al. TMPRSS2 and TMPRSS4 promote SARS-CoV-2 infection of human small intestinal enterocytes. *Sci. Immunol.* **5**, eabc3582 (2020).
- Stadlbauer, D. et al. SARS-CoV-2 seroconversion in humans: a detailed protocol for a serological assay, antigen production, and test setup. *Curr. Protoc. Microbiol.* **57**, e100 (2020).
- Fairhead, M. & Howarth, M. Site-specific biotinylation of purified proteins using BirA. *Methods Mol. Biol.* **1266**, 171–184 (2015).
- Chen, R. E. et al. Resistance of SARS-CoV-2 variants to neutralization by monoclonal and serum-derived polyclonal antibodies. *Nat. Med.* **27**, 717–726 (2021).
- VanBlargan, L. A. et al. A potentially neutralizing SARS-CoV-2 antibody inhibits variants of concern by utilizing unique binding residues in a highly conserved epitope. *Immunity* **54**, 2399–2416.e6 (2021).
- Mudd, P. A. et al. SARS-CoV-2 mRNA vaccination elicits a robust and persistent T follicular helper cell response in humans. *Cell* **185**, 603–613.e15 (2022).
- Wrarmert, J. et al. Broadly cross-reactive antibodies dominate the human B cell response against 2009 pandemic H1N1 influenza virus infection. *J. Exp. Med.* **208**, 181–193 (2011).
- Smith, K. et al. Rapid generation of fully human monoclonal antibodies specific to a vaccinating antigen. *Nat. Protoc.* **4**, 372–384 (2009).
- Wrarmert, J. et al. Rapid cloning of high-affinity human monoclonal antibodies against influenza virus. *Nature* **453**, 667–671 (2008).
- Nachbagauer, R. et al. Broadly reactive human monoclonal antibodies elicited following pandemic H1N1 influenza virus exposure protect mice against highly pathogenic H5N1 challenge. *J. Virol.* **92**, 1–17 (2018).
- Brochet, X., Lefranc, M.-P. & Giudicelli, V. IMGT/V-QUEST: the highly customized and integrated system for IG and TR standardized V-J and V-D-J sequence analysis. *Nucleic Acids Res.* **36**, W503–W508 (2008).

57. Giudicelli, V., Brochet, X. & Lefranc, M.-P. IMGT/V-QUEST: IMGT standardized analysis of the immunoglobulin (IG) and T cell receptor (TR) nucleotide sequences. *Cold Spring Harb. Protoc.* **2011**, pdb.prot5633 (2011).
58. Vander Heiden, J. A. et al. pRESTO: a toolkit for processing high-throughput sequencing raw reads of lymphocyte receptor repertoires. *Bioinformatics* **30**, 1930–1932 (2014).
59. Ye, J., Ma, N., Madden, T. L. & Ostell, J. M. IgBLAST: an immunoglobulin variable domain sequence analysis tool. *Nucleic Acids Res.* **41**, W34–W40 (2013).
60. Gadala-Maria, D., Yaari, G., Uduman, M. & Kleinstein, S. H. Automated analysis of high-throughput B-cell sequencing data reveals a high frequency of novel immunoglobulin V gene segment alleles. *Proc. Natl Acad. Sci. USA* **112**, E862–E870 (2015).
61. Gupta, N. T. et al. Change-O: a toolkit for analyzing large-scale B cell immunoglobulin repertoire sequencing data. *Bioinformatics* **31**, 3356–3358 (2015).
62. Gu, Z., Gu, L., Eils, R., Schlesner, M. & Brors, B. circlize implements and enhances circular visualization in R. *Bioinformatics* **30**, 2811–2812 (2014).
63. Wolf, F. A., Angerer, P. & Theis, F. J. SCANPY: large-scale single-cell gene expression data analysis. *Genome Biol.* **19**, 15 (2018).
64. Haebe, S. et al. Single-cell analysis can define distinct evolution of tumor sites in follicular lymphoma. *Blood* **137**, 2869–2880 (2021).
65. Mourcin, F. et al. Follicular lymphoma triggers phenotypic and functional remodeling of the human lymphoid stromal cell landscape. *Immunity* **54**, 1788–1806.e7 (2021).

**Acknowledgements** The authors thank all the donors for generously providing precious specimens; L. Kessels and the Washington University School of Medicine 382 Study Team (study coordinators A. Haile, R. Thompson, D. Carani, K. Gray and C. Ayres; pharmacists M. Royal and J. Tran; and laboratory technicians L. Blair, A. Afghanzada and N. Schodl) for assistance with scheduling participants and sample collection; P. Woodard, B. Thomas, M. Harrod, R. Hamlin, M. Rohn; the staff of the Center for Clinical Research Imaging at Washington University School of Medicine for assistance with sample collection; and C. Dalton and B. Roemmich for performing the nucleocapsid binding assay. The WU382 study was reviewed and approved by the Washington University Institutional Review Board (approval no. 202109021). This work was supported in part with funding from the US National Institutes of Health (NIH) and Moderna. The Ellebedy laboratory was supported by NIH grants U01AI141990, 1U01AI150747, 5U01AI144616-02 and R01AI168178-01. The Diamond laboratory was supported by NIH grant R01 AI157155. The Whelan laboratory was supported by NIH grant R01 AI163019. The content of this manuscript is solely the responsibility of the authors and does not necessarily represent the official view of NIAID or NIH.

**Author contributions** A.H.E., J.A.O., R.M.P., R.P., B.N. and S.C. conceived and designed the study. J.A.O., M.K.K. and R.M.P. wrote and maintained the IRB protocol, recruited participants and coordinated sample collection. W.B.A., W.K., F.H. and J.S.T. processed specimens. W.B.A.,

S.K.M., S.F.M. and J.S.T. performed multiplex bead array and ELISA. W.B.A., F.H. and J.S.T. performed ELISpot. W.B.A., S.K.M. and S.M. performed VSV neutralization assays. W.B.A., S.K.M., W.K., A. J. Schmitz, T.L., S.C.H., A. J. Sturtz, K.M.M., B.E., I.F.F. and J.S.T. generated and characterized monoclonal antibodies. J.Q.Z. analysed scRNA-seq and BCR repertoire data. Z.L. rescued and produced the chimeric vesicular stomatitis viruses for neutralization assays and performed and analysed epitope mapping. B.Y. performed the SARS-CoV-2 virus neutralization assays. W.K. and A. J. Sturtz prepared libraries for scRNA-seq. A. J. Schmitz performed RNA extractions and library preparation for BCR bulk sequencing and expressed SARS-CoV-2 S and variant proteins. S.M.S. generated the authentic SARS-CoV-2 virus stocks. C.W.F. supervised the nucleocapsid binding assay. I.P. supervised bone marrow specimen collection. B.S.S. and W.D.M. performed FNA. B.S.S., W.D.M. and S.A.T. supervised lymph node evaluation prior to FNA and specimen collection and evaluated lymph node ultrasound data. J.S.T. sorted cells and collected and analysed the flow cytometry data. L.P.-R., R.P., R.N., J.S.T. and A.H.E. analysed data. A.H.E., M.S.D. and S.P.J.W. supervised experiments and obtained funding. J.S.T. and A.H.E. composed the manuscript. All authors reviewed and edited the manuscript.

**Competing interests** The Ellebedy laboratory and Infectious Disease Clinical Research Unit has received funding under sponsored research agreements from Moderna related to the data presented in the current study. The Ellebedy laboratory received funding from Emergent BioSolutions and AbbVie that are unrelated to the data presented in the current study. A.H.E. has received consulting and speaking fees from InBios International, Fimbrion Therapeutics, RGAX, Mubadala Investment Company, Moderna, Pfizer, GSK, Danaher, Third Rock Ventures, Goldman Sachs and Morgan Stanley and is the founder of ImmuneBio Consulting. W.B.A., A. J. Schmitz, S.P.J.W., M.S.D., J.S.T. and A.H.E. are recipients of a licensing agreement with Abbvie that is unrelated to the data presented in the current study. M.S.D. is a consultant for Inbios, Vir Biotechnology, Senda Biosciences, Moderna, Sterne-Kessler and Immunome. The Diamond laboratory has received unrelated funding support in sponsored research agreements from Vir Biotechnology, Emergent BioSolutions and Moderna. S.P.J.W. is a consultant for Thylacine Bio. S.P.J.W. is a recipient of a licensing agreement with Vir Biotechnology and Merck. The Whelan laboratory has received unrelated funding support in sponsored research agreements from Vir Biotechnology. R.P., B.N., S.C. and R.N. are employees of and shareholders in Moderna. The other authors declare no competing interests.

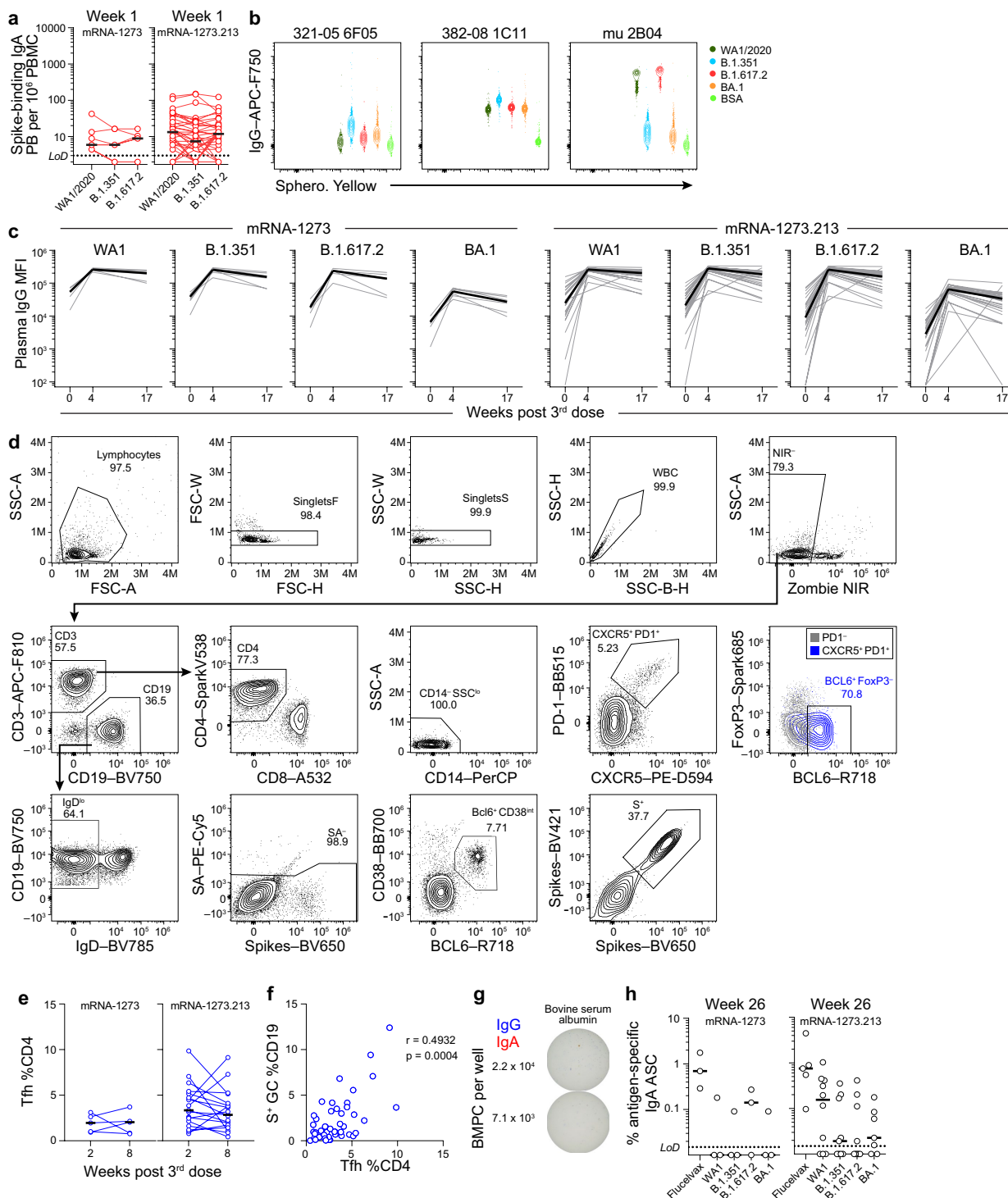
#### Additional information

**Supplementary information** The online version contains supplementary material available at <https://doi.org/10.1038/s41586-023-06025-4>.

**Correspondence and requests for materials** should be addressed to Jackson S. Turner or Ali H. Ellebedy.

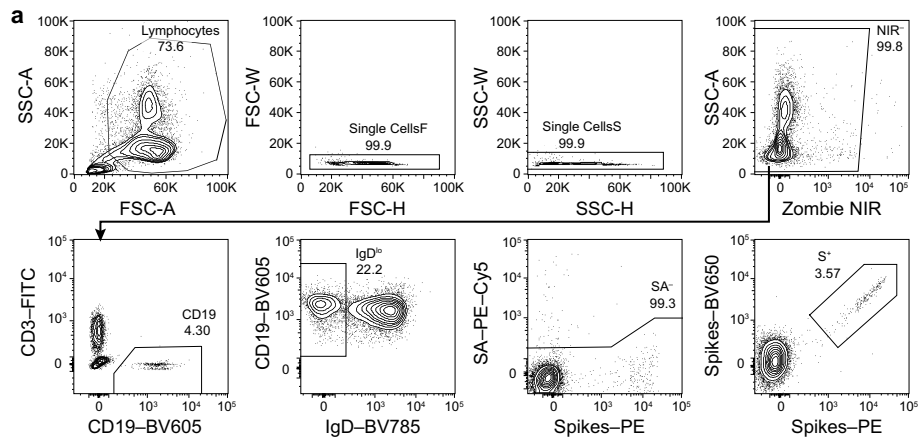
**Peer review information** *Nature* thanks Sophie Valkenburg and the other, anonymous, reviewer(s) for their contribution to the peer review of this work. Peer review reports are available.

**Reprints and permissions information** is available at <http://www.nature.com/reprints>.

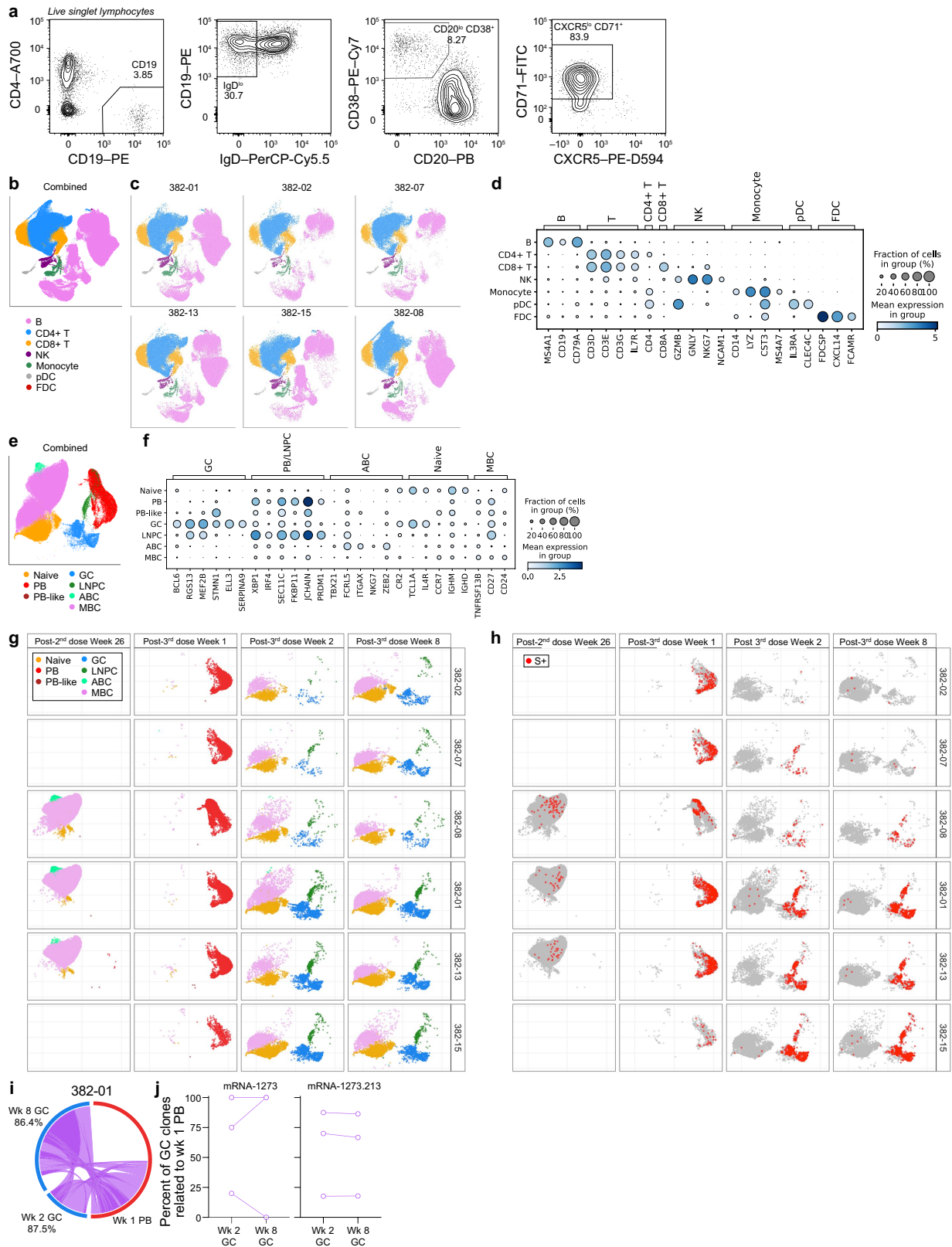


**Extended Data Fig. 1 | Robust GC and Tfh responses to mRNA-1273 and mRNA-1273.213 boosters.** (a) Frequencies of IgA plasmablasts specific for the indicated antigens measured by ELISpot in week-1 PBMC from participants who received mRNA-1273 (left) and mRNA-1273.213 (right). (b) Flow cytometry plots of influenza B/HA-specific mAb 321-05 6F05<sup>34</sup>, cross-reactive mAb 382-08 1C11, and residue E484-specific mAb mu 2B04<sup>42</sup> binding to indicated strains of SARS-CoV-2 by multiplex bead binding array. (c) Plasma IgG binding to indicated strains of SARS-CoV-2 measured by multiplex bead binding array in participants who received mRNA-1273 (left) and mRNA-1273.213 (right). (d) Gating strategy for analyzing S<sup>+</sup> germinal centre B cells and T follicular

helper cells (T<sub>FH</sub>) in FNA. (e) Frequencies of T<sub>FH</sub> from FNA of draining lymph nodes. (f) Correlation between frequencies of S<sup>+</sup> germinal centre B cells and T<sub>FH</sub>.  $P$  and  $r$  values from two-sided Spearman test. (g) Representative ELISpot wells coated with BSA, and developed in blue (IgG) and red (IgA) after plating the indicated numbers of BMPCs. (h) Frequencies of IgA-secreting BMPCs specific for the indicated antigens 26 weeks post-boost. Black lines indicate medians. Symbols at each time point represent one sample. For mRNA-1273 and mRNA-1273.213 respectively,  $n = 7$  and 38 (a),  $n = 6$  and 28 (c),  $n = 5$  and 20 (e),  $n = 3$  and 10 (h).

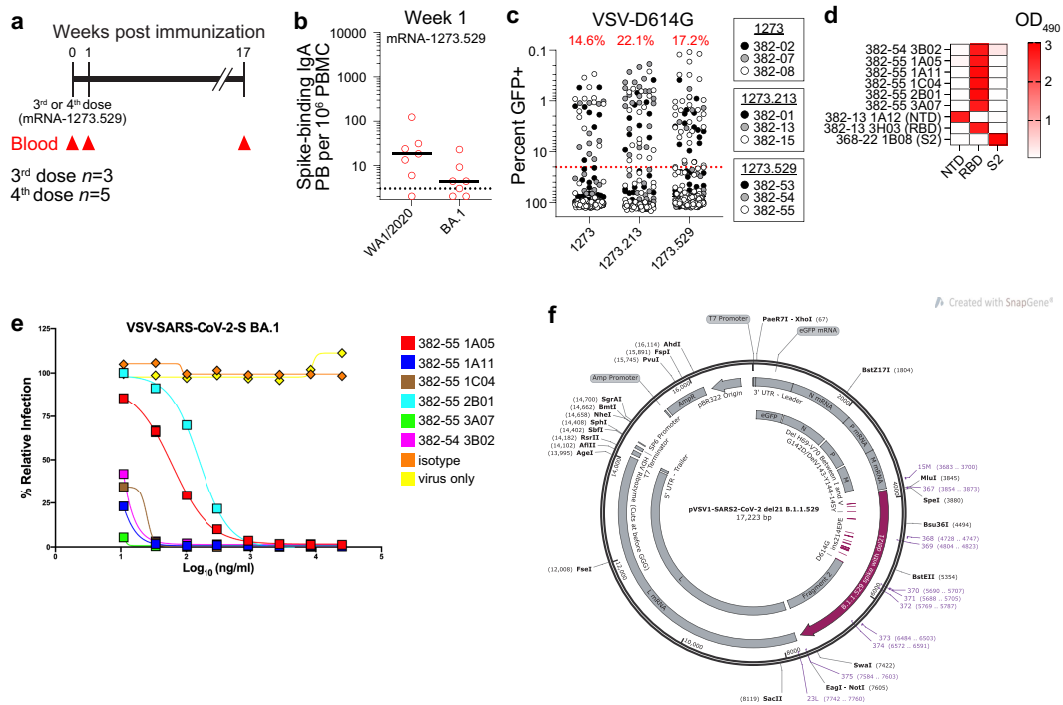


**Extended Data Fig. 2 | Breadth of MBC-derived mAbs after mRNA-1273 and mRNA-1273.213 boosters. (a) Gating strategy for sorting S<sup>+</sup> MBC from PBMC.**



**Extended Data Fig. 3 | Maturation of S-specific MBCs in response to mRNA-1273 or mRNA-1273.213 booster. (a)** Gating strategy for sorting plasmablasts from PBMC. **(b, c, e, g)** UMAPs showing scRNA-seq transcriptional clusters of total cells (b, c) or B cells (e, g) from all participants (b, e) or from each participant separately (c, g). **(d, f)** Dot plots for the marker genes used for identifying the annotated clusters in (b, c) (d) and in (e, g) (f). **(h)** SARS-CoV-2 S-specific clones visualized in red on UMAPs of B cells from each participant separately and faceted by time point. **(i)** Clonal overlap between S-binding

plasmablasts and germinal centre B cells at indicated time points. Arc length corresponds to the number of BCR sequences and chord width corresponds to clone size. Purple chords correspond to clones spanning both compartments. Percentages are of germinal centre B cell clones related to plasmablasts at each time point. **(j)** Percentages of S-specific germinal centre clones related to week 1 plasmablasts. Symbols at each time point represent one sample,  $n = 3$  for mRNA-1273 and  $n = 3$  for mRNA-1273.213.



**Extended Data Fig. 4 | Characterization of BA.1-specific mAbs.** (a) Study design for mRNA-1273.529 vaccine cohort. Three and five healthy adult volunteers were enrolled and received an mRNA-1273.529 booster as a third or fourth dose, respectively. Blood was collected at baseline and at 1 and 17 weeks post-boost. (b) Frequencies of S-binding IgA-producing plasmablasts in PBMC 1 week post-boost measured by ELISpot in participants who received mRNA-1273.529. Black lines indicate medians. Symbols represent one sample;  $n = 7$ . (c) Neutralizing activity of mAbs from week 17 S<sup>+</sup> MBCs against chimeric vesicular stomatitis virus in which the native envelope glycoprotein was replaced with S from WA1/2020 (with D614G mutation). Each symbol represents one

mAb,  $n = 205$  for mRNA-1273,  $n = 222$  for mRNA-1273.213, and  $n = 303$  for mRNA-1273.529. Percentages are of mAbs above the 80% infection reduction threshold. (d) Binding of mAbs to constituent domains of BA.1S by ELISA performed in duplicate, presented as mean OD<sub>490</sub> values. S2-specific mAb 368-22 1B08 was described previously<sup>2</sup>. (e) Titration of mAbs to determine neutralizing concentrations against chimeric vesicular stomatitis virus in which the native envelope glycoprotein was replaced with S from SARS-CoV-2 BA.1. Data are representative of two independent experiments. (f) Plasmid map for chimeric vesicular stomatitis virus in which the native envelope glycoprotein was replaced with S from BA.1 with primers indicated in purple.



# Article

Extended Data Table 1 | Study WU382 participant demographics

Variable	Total n=54 n (%)
<b>Age (median [range])</b>	37.5 (18-72)
<b>Sex</b>	
Female	31 (57.4)
Male	23 (42.6)
<b>Race</b>	
White	49 (90.7)
Black	2 (3.7)
Asian	2 (3.7)
Other	1 (1.9)
<b>Ethnicity</b>	
Not of Hispanic, Latinx, or Spanish origin	52 (96.3)
Hispanic, Latinx, Spanish origin	2 (3.7)
<b>BMI (median [range])</b>	26.86 (19.3-47.74)
<b>Comorbidities</b>	
Lung disease	1 (1.9)
Diabetes mellitus	1 (1.9)
Hypertension	10 (18.5)
Cardiovascular	0 (0)
Liver disease	0 (0)
Chronic kidney disease	0 (0)
Cancer on chemotherapy	0 (0)
Hematological malignancy	0 (0)
Pregnancy	0 (0)
Neurological	0 (0)
Rheumatologic disease	0 (0)
HIV	0 (0)
Solid organ transplant recipient	0 (0)
Bone marrow transplant recipient	0 (0)
Hyperlipidemia	2 (3.7)
<b>Type of baseline vaccine</b>	
Pfizer	29 (53.7)
Moderna	25 (46.3)
<b>Type of booster vaccine (3<sup>rd</sup> dose)</b>	
Moderna mRNA-1273	12 (22.2)
Moderna mRNA-1273.213	39 (72.2)
Moderna mRNA-1273.529	3 (6)
<b>Time from second dose to booster in days (median [range])</b>	272.5 (196-356)
<b>Participants who received 2<sup>nd</sup> booster (4<sup>th</sup> dose)</b>	<b>5 (9)</b>
Moderna 1273.529	5 (9)

Proportion of participants in indicated demographic categories.

**Extended Data Table 2 | Booster (3<sup>rd</sup> or 4<sup>th</sup> dose) vaccine side effects<sup>a</sup>**

<b>Side effects from booster vaccines</b>	<b>Overall (n=54)</b>	<b>mRNA-1273.213 (n=39)</b>	<b>mRNA-1273.529 (n=3)</b>	<b>mRNA-1273 (n=12)</b>
Chills	24 (44.4)	21 (53.8)	0 (0)	2 (28.6)
Feeling unwell	29 (53.7)	25 (64.1)	1 (33.3)	3 (25)
Fever	15 (27.8)	14 (35.9)	0 (0)	1 (14.3)
Headache	25 (46.3)	20 (51.3)	1 (33.3)	1 (14.3)
Injection site pain	40 (74.1)	29 (74.4)	1 (33.3)	6 (85.7)
Injection site swelling	5 (9.3)	5 (12.8)	0 (0)	0 (0)
Injection site redness	7 (13)	6 (15.4)	0 (0)	1 (8.3)
Joint pain	13 (24.1)	10 (25.6)	0 (0)	3 (25)
Muscle pain	24 (44.4)	19 (48.7)	1 (33.3)	4 (33.3)
Nausea	10 (18.5)	8 (20.5)	1 (33.3)	1 (8.3)
Swollen lymph nodes	14 (25.9)	10 (25.6)	0 (0)	4 (25.6)
Tiredness	36 (66.7)	27 (69.2)	1 (33.3)	8 (66.7)

<sup>a</sup>These data are reported for a subset of the participants enrolled in a parallel clinical trial (NCT04927065) who provided additional consent for the collection of samples in this study. Safety and reactogenicity data for all participants in the clinical trial are reported separately<sup>22</sup>.

# Article

**Extended Data Table 3 | Processing of BCR reads from bulk-seq**

Participant	Timepoint (post-3 <sup>rd</sup> dose)	Tissue	Sorting	Cell Count	Sequence Count			
					Input Reads	Preprocessed Reads	Post-QC Productive Heavy Chains	Unique Heavy Chain VDJs
382-01	Week 17	Blood	IgDlo	111946	1583322	44815	38187	17282
382-01	Week 26	BM	BMPC	100000	1758531	108513	98986	56058
382-02	Week 17	Blood	IgDlo	117796	1814249	31690	27361	14377
382-02	Week 26	BM	BMPC	500000	1753509	92329	79291	35369
382-07	Week 17	Blood	IgDlo	40722	1472130	7494	6028	4180
382-07	Week 26	BM	BMPC	100000	931929	44883	40802	20350
382-08	Week 17	Blood	IgDlo	225941	1640142	38798	33787	19143
382-08	Week 26	BM	BMPC	500000	1413927	76177	68170	39745
382-13	Week 2	LN	GC B	1457	391576	120	81	48
382-13	Week 2	LN	LNPC	510	1177974	639	456	247
382-13	Week 8	LN	GC B	361	845333	54	28	23
382-13	Week 8	LN	LNPC	75	762774	144	101	50
382-13	Week 17	Blood	IgDlo	100067	1883825	28252	24250	13743
382-13	Week 26	BM	BMPC	500000	833430	34145	31654	23740
382-15	Week 2	LN	GC B	10851	1092056	843	539	393
382-15	Week 2	LN	LNPC	1261	1443988	3062	2300	833
382-15	Week 8	LN	GC B	8218	1123859	699	452	294
382-15	Week 8	LN	LNPC	2943	1457122	3496	2419	1178
382-15	Week 17	Blood	IgDlo	192652	927478	30426	26818	16746
382-15	Week 26	BM	BMPC	440000	960553	48008	44795	28188
382-53	Week 17	Blood	IgDlo	219910	1273447	65305	50662	19066
382-54	Week 1	Blood	PB	14107	1359995	32452	28136	9899
382-54	Week 8	LN	GC B	420	1796016	154	73	41
382-54	Week 8	LN	LNPC	97	890863	281	207	103
382-54	Week 17	Blood	IgDlo	119119	1406118	58308	48507	18553
382-55	Week 1	Blood	PB	28596	1498648	57378	49948	19062
382-55	Week 17	Blood	IgDlo	97942	1586896	50695	42233	19154

Numbers of cells and reads from bulk-sorted specimens at indicated timepoints post-vaccination.

**Extended Data Table 4 | Processing of BCR and 5' gene expression data from scRNA-seq. NS=no sorting**

Participant	Timepoint (post-3 <sup>rd</sup> dose unless noted)	Tissue	Sorting	Replicate	BCR		5' Gene Expression			
					Pre-QC number of cells	Post-QC number of cells	Pre-QC number of cells	Post-QC number of cells	Median number of UMIs per cell	Median number of genes per cell
382-01	Post-2 <sup>nd</sup> dose Week 26	Blood	IgDlo	1	10056	7702	10574	10491	3523	1364
382-01	Post-2 <sup>nd</sup> dose Week 26	Blood	IgDlo	2	9590	7400	10020	9946	3568.5	1369
382-01	Week 1	Blood	PB	1	3582	2939	3829	3004	6819	1605
382-01	Week 2	LN	NS	1	2974	2704	7235	6725	3006	1214
382-01	Week 2	LN	NS	2	3275	2962	7595	7138	3093	1240
382-01	Week 2	LN	NS	3	3158	2821	7553	7013	3066	1220
382-01	Week 2	LN	NS	4	3132	2770	7111	6594	3096	1227
382-01	Week 8	LN	NS	1	2445	2265	7753	7468	3124.5	1276
382-01	Week 8	LN	NS	2	2295	2109	7469	7160	3152	1299
382-01	Week 8	LN	NS	3	2331	2130	7835	7542	3144	1293.5
382-01	Week 8	LN	NS	4	2545	2283	8039	7744	3067	1247
382-02	Week 1	Blood	PB	1	2560	2077	2588	2189	6548	1511
382-02	Week 2	LN	NS	1	1615	1523	8901	8172	3541	1394
382-02	Week 8	LN	NS	1	5863	4915	8689	8271	3546	1396
382-02	Week 8	LN	NS	2	5241	4548	8895	8430	3514	1392
382-07	Week 1	Blood	PB	1	3104	2177	2437	1764	6987.5	1521
382-07	Week 2	LN	NS	1	2234	2108	8886	8353	3326	1345
382-07	Week 8	LN	NS	1	2774	2590	9967	9314	3365.5	1438
382-07	Week 8	LN	NS	2	2656	2473	9691	9002	3382	1443
382-08	Post-2 <sup>nd</sup> dose Week 26	Blood	IgDlo	1	13540	11447	13727	13680	3355.5	1319
382-08	Post-2 <sup>nd</sup> dose Week 26	Blood	IgDlo	2	13224	11278	13538	13478	3423	1345
382-08	Week 1	Blood	PB	1	10513	7295	9029	8331	821	368
382-08	Week 1	Blood	PB	2	2347	1008	725	512	7148.5	1593.5
382-08	Week 2	LN	NS	1	1704	1566	6509	6232	3288	1313
382-08	Week 2	LN	NS	2	1686	1551	6302	6003	3292	1295
382-08	Week 8	LN	NS	1	942	865	7714	6784	3369	1497
382-08	Week 8	LN	NS	2	908	852	7915	6988	3355	1482
382-13	Post-2 <sup>nd</sup> dose Week 26	Blood	IgDlo	1	9246	7601	9534	9483	3314	1283
382-13	Post-2 <sup>nd</sup> dose Week 26	Blood	IgDlo	2	8557	7183	8737	8674	3628	1350
382-13	Week 1	Blood	PB	1	3755	3124	3945	3377	6256	1540
382-13	Week 2	LN	NS	1	1481	1378	5735	4801	3048	1341
382-13	Week 2	LN	NS	2	1527	1390	6257	5288	2911.5	1294
382-13	Week 8	LN	NS	1	3955	3697	16565	15153	3263	1433
382-13	Week 8	LN	NS	2	4002	3740	15887	14582	3247	1440
382-15	Week 1	Blood	PB	1	4999	2755	948	695	6055	1489
382-15	Week 2	LN	NS	1	4516	4130	10731	8792	3267	1437.5
382-15	Week 2	LN	NS	2	4440	4060	10589	8680	3327	1452
382-15	Week 8	LN	NS	1	14533	11681	24234	23756	1684	974
382-15	Week 8	LN	NS	2	5135	4568	13272	10633	3174	1367

Numbers of cells and reads from scRNAseq for indicated specimens at indicated timepoints post-vaccination.

# Article

**Extended Data Table 5 | Cell counts and frequencies of overall and B cell transcriptional clusters from scRNA-seq**

Participant	Transcriptional Cluster						
	B	CD4+ T	CD8+ T	NK	Monocyte	pDC	FDC
382-01	43604 (54.1%)	27552 (34.2%)	6663 (8.3%)	1114 (1.4%)	1260 (1.6%)	452 (0.6%)	6 (0%)
382-02	8722 (32.2%)	14566 (53.9%)	2796 (10.3%)	249 (0.9%)	546 (2%)	155 (0.6%)	11 (0%)
382-07	8982 (31.6%)	15493 (54.5%)	2645 (9.3%)	566 (2%)	494 (1.7%)	246 (0.9%)	5 (0%)
382-08	40884 (65.9%)	15078 (24.3%)	4685 (7.6%)	652 (1.1%)	432 (0.7%)	266 (0.4%)	1 (0%)
382-13	31918 (52%)	22362 (36.4%)	5976 (9.7%)	507 (0.8%)	485 (0.8%)	107 (0.2%)	1 (0%)
382-15	34299 (65.3%)	13031 (24.8%)	3466 (6.6%)	972 (1.8%)	633 (1.2%)	143 (0.3%)	12 (0%)
Combined	168409 (54%)	108082 (34.6%)	26231 (8.4%)	4060 (1.3%)	3850 (1.2%)	1369 (0.4%)	36 (0%)

Participant	Timepoint (post-3 <sup>rd</sup> dose unless noted)	B cell transcriptional cluster						
		GC	LNPC	PB	PB-like	ABC	Naive	MBC
382-01	Post-2nd dose week 26	0 (0%)	0 (0%)	0 (0%)	1 (0%)	470 (2.3%)	96 (0.5%)	19674 (97.2%)
382-01	Week 1	0 (0%)	0 (0%)	2600 (99.4%)	0 (0%)	0 (0%)	3 (0.1%)	13 (0.5%)
382-01	Week 2	1184 (11.1%)	269 (2.5%)	0 (0%)	0 (0%)	9 (0.1%)	3619 (34%)	5569 (52.3%)
382-01	Week 8	1228 (14.5%)	226 (2.7%)	0 (0%)	0 (0%)	0 (0%)	1848 (21.7%)	5195 (61.1%)
382-01	Combined	2412 (5.7%)	495 (1.2%)	2600 (6.2%)	1 (0%)	479 (1.1%)	5566 (13.3%)	30451 (72.5%)
382-02	Week 1	0 (0%)	0 (0%)	1805 (99.1%)	1 (0.1%)	0 (0%)	6 (0.3%)	10 (0.5%)
382-02	Week 2	68 (4.9%)	19 (1.4%)	0 (0%)	0 (0%)	0 (0%)	720 (51.6%)	588 (42.2%)
382-02	Week 8	364 (7.5%)	52 (1.1%)	0 (0%)	0 (0%)	0 (0%)	1639 (33.6%)	2830 (57.9%)
382-02	Combined	432 (5.3%)	71 (0.9%)	1805 (22.3%)	1 (0%)	0 (0%)	2365 (29.2%)	3428 (42.3%)
382-07	Week 1	0 (0%)	0 (0%)	1438 (98.9%)	0 (0%)	1 (0.1%)	4 (0.3%)	11 (0.8%)
382-07	Week 2	81 (4.1%)	68 (3.5%)	0 (0%)	0 (0%)	1 (0.1%)	943 (48%)	871 (44.3%)
382-07	Week 8	425 (8.8%)	69 (1.4%)	0 (0%)	0 (0%)	0 (0%)	1403 (29.1%)	2917 (60.6%)
382-07	Combined	506 (6.1%)	137 (1.7%)	1438 (17.5%)	0 (0%)	2 (0%)	2350 (28.5%)	3799 (46.1%)
382-08	Post-2nd dose week 26	0 (0%)	0 (0%)	0 (0%)	1 (0%)	297 (1.1%)	246 (0.9%)	26601 (98%)
382-08	Week 1	0 (0%)	0 (0%)	8771 (99.7%)	1 (0%)	0 (0%)	0 (0%)	29 (0.3%)
382-08	Week 2	157 (5.7%)	75 (2.7%)	0 (0%)	0 (0%)	3 (0.1%)	1281 (46.6%)	1235 (44.9%)
382-08	Week 8	161 (9.6%)	57 (3.4%)	0 (0%)	0 (0%)	0 (0%)	739 (44.2%)	715 (42.8%)
382-08	Combined	318 (0.8%)	132 (0.3%)	8771 (21.7%)	2 (0%)	300 (0.7%)	2266 (5.6%)	28580 (70.8%)
382-13	Post-2nd dose week 26	0 (0%)	0 (0%)	7 (0%)	2 (0%)	45 (0.2%)	109 (0.6%)	17940 (99.1%)
382-13	Week 1	0 (0%)	0 (0%)	2714 (98.7%)	3 (0.1%)	0 (0%)	9 (0.3%)	23 (0.8%)
382-13	Week 2	913 (31.4%)	339 (11.7%)	0 (0%)	0 (0%)	0 (0%)	877 (30.2%)	777 (26.7%)
382-13	Week 8	873 (13.6%)	116 (1.8%)	0 (0%)	0 (0%)	0 (0%)	2478 (38.5%)	2968 (46.1%)
382-13	Combined	1786 (5.9%)	455 (1.5%)	2721 (9.0%)	5 (0%)	45 (0.1%)	3473 (11.5%)	21708 (71.9%)
382-15	Week 1	0 (0%)	0 (0%)	562 (93.4%)	1 (0.2%)	0 (0%)	2 (0.3%)	37 (6.1%)
382-15	Week 2	1223 (16.1%)	173 (2.3%)	0 (0%)	0 (0%)	0 (0%)	3013 (39.8%)	3170 (41.8%)
382-15	Week 8	990 (16.8%)	298 (5.1%)	0 (0%)	0 (0%)	2 (0%)	2722 (46.2%)	1881 (31.9%)
382-15	Combined	2213 (15.7%)	471 (3.3%)	562 (4.0%)	1 (0%)	2 (0%)	5737 (40.8%)	5088 (36.2%)
Combined		7667 (5.4%)	1761 (1.2%)	17897 (12.5%)	10 (0%)	828 (0.6%)	21757 (15.2%)	93054 (65.1%)

Numbers and frequencies of transcriptionally-defined cell populations from scRNAseq of indicated specimens at indicated timepoints post-vaccination.

**Extended Data Table 6 | Counts of B cells found in S-binding clones and frequencies out of respective B cell transcriptional clusters**

Participant	Timepoint (post-3 <sup>rd</sup> dose unless noted)	B cell transcriptional cluster						
		GC	LNPC	PB	PB-like	ABC	Naive	MBC
382-01	Post-2nd dose week 26	0 (-)	0 (-)	0 (-)	0 (0%)	1 (0.2%)	0 (0%)	30 (0.2%)
382-01	Week 1	0 (-)	0 (-)	484 (18.6%)	0 (-)	0 (-)	0 (0%)	0 (0%)
382-01	Week 2	125 (10.6%)	74 (27.5%)	0 (-)	0 (-)	0 (0%)	2 (0.1%)	9 (0.2%)
382-01	Week 8	315 (25.7%)	72 (31.9%)	0 (-)	0 (-)	0 (-)	0 (0%)	4 (0.1%)
382-01	Combined	440 (18.2%)	146 (29.5%)	484 (18.6%)	0 (0%)	1 (0.2%)	2 (0%)	43 (0.1%)
382-02	Week 1	0 (-)	0 (-)	149 (8.3%)	0 (0%)	0 (-)	0 (0%)	0 (0%)
382-02	Week 2	1 (1.5%)	1 (5.3%)	0 (-)	0 (-)	0 (-)	0 (0%)	0 (0%)
382-02	Week 8	1 (0.3%)	0 (0%)	0 (-)	0 (-)	0 (-)	0 (0%)	4 (0.1%)
382-02	Combined	2 (0.5%)	1 (1.4%)	149 (8.3%)	0 (0%)	0 (-)	0 (0%)	4 (0.1%)
382-07	Week 1	0 (-)	0 (-)	192 (13.4%)	0 (-)	0 (0%)	0 (0%)	0 (0%)
382-07	Week 2	22 (27.2%)	15 (22.1%)	0 (-)	0 (-)	0 (0%)	0 (0%)	1 (0.1%)
382-07	Week 8	3 (0.7%)	0 (0%)	0 (-)	0 (-)	0 (-)	0 (0%)	3 (0.1%)
382-07	Combined	25 (4.9%)	15 (10.9%)	192 (13.4%)	0 (-)	0 (0%)	0 (0%)	4 (0.1%)
382-08	Post-2nd dose week 26	0 (-)	0 (-)	0 (-)	0 (0%)	2 (0.7%)	0 (0%)	74 (0.3%)
382-08	Week 1	0 (-)	0 (-)	184 (2.1%)	0 (0%)	0 (-)	0 (-)	0 (0%)
382-08	Week 2	35 (22.3%)	8 (10.7%)	0 (-)	0 (-)	0 (0%)	0 (0%)	2 (0.2%)
382-08	Week 8	48 (29.8%)	10 (17.5%)	0 (-)	0 (-)	0 (-)	0 (0%)	0 (0%)
382-08	Combined	83 (26.1%)	18 (13.6%)	184 (2.1%)	0 (0%)	2 (0.7%)	0 (0%)	76 (0.3%)
382-13	Post-2nd dose week 26	0 (-)	0 (-)	0 (0%)	0 (0%)	0 (0%)	0 (0%)	31 (0.2%)
382-13	Week 1	0 (-)	0 (-)	270 (9.9%)	0 (0%)	0 (-)	0 (0%)	0 (0%)
382-13	Week 2	157 (17.2%)	75 (22.1%)	0 (-)	0 (-)	0 (-)	0 (0%)	0 (0%)
382-13	Week 8	192 (22%)	69 (59.5%)	0 (-)	0 (-)	0 (-)	0 (0%)	3 (0.1%)
382-13	Combined	349 (19.5%)	144 (31.6%)	270 (9.9%)	0 (0%)	0 (0%)	0 (0%)	34 (0.2%)
382-15	Week 1	0 (-)	0 (-)	27 (4.8%)	0 (0%)	0 (-)	0 (0%)	0 (0%)
382-15	Week 2	403 (33%)	33 (19.1%)	0 (-)	0 (-)	0 (-)	3 (0.1%)	1 (0%)
382-15	Week 8	370 (37.4%)	131 (44%)	0 (-)	0 (-)	0 (0%)	2 (0.1%)	5 (0.3%)
382-15	Combined	773 (34.9%)	164 (34.8%)	27 (4.8%)	0 (0%)	0 (0%)	5 (0.1%)	6 (0.1%)
Combined		1672 (21.8%)	488 (27.7%)	1306 (7.3%)	0 (0%)	3 (0.4%)	7 (0%)	167 (0.2%)

Numbers and frequencies of S-binding B cells among transcriptionally-defined cell populations from scRNAseq of indicated specimens at indicated timepoints post-vaccination.

## Reporting Summary

Nature Portfolio wishes to improve the reproducibility of the work that we publish. This form provides structure for consistency and transparency in reporting. For further information on Nature Portfolio policies, see our [Editorial Policies](#) and the [Editorial Policy Checklist](#).

### Statistics

For all statistical analyses, confirm that the following items are present in the figure legend, table legend, main text, or Methods section.

- | n/a                                 | Confirmed  |
|-------------------------------------|--|
| <input type="checkbox"/>            | <input checked="" type="checkbox"/> The exact sample size ( $n$ ) for each experimental group/condition, given as a discrete number and unit of measurement  |
| <input type="checkbox"/>            | <input checked="" type="checkbox"/> A statement on whether measurements were taken from distinct samples or whether the same sample was measured repeatedly  |
| <input type="checkbox"/>            | <input checked="" type="checkbox"/> The statistical test(s) used AND whether they are one- or two-sided<br><i>Only common tests should be described solely by name; describe more complex techniques in the Methods section.</i>   |
| <input checked="" type="checkbox"/> | <input type="checkbox"/> A description of all covariates tested  |
| <input type="checkbox"/>            | <input checked="" type="checkbox"/> A description of any assumptions or corrections, such as tests of normality and adjustment for multiple comparisons  |
| <input type="checkbox"/>            | <input checked="" type="checkbox"/> A full description of the statistical parameters including central tendency (e.g. means) or other basic estimates (e.g. regression coefficient) AND variation (e.g. standard deviation) or associated estimates of uncertainty (e.g. confidence intervals) |
| <input type="checkbox"/>            | <input checked="" type="checkbox"/> For null hypothesis testing, the test statistic (e.g. $F$ , $t$ , $r$ ) with confidence intervals, effect sizes, degrees of freedom and $P$ value noted<br><i>Give <math>P</math> values as exact values whenever suitable.</i>                            |
| <input checked="" type="checkbox"/> | <input type="checkbox"/> For Bayesian analysis, information on the choice of priors and Markov chain Monte Carlo settings  |
| <input checked="" type="checkbox"/> | <input type="checkbox"/> For hierarchical and complex designs, identification of the appropriate level for tests and full reporting of outcomes  |
| <input type="checkbox"/>            | <input checked="" type="checkbox"/> Estimates of effect sizes (e.g. Cohen's $d$ , Pearson's $r$ ), indicating how they were calculated   |

*Our web collection on [statistics for biologists](#) contains articles on many of the points above.*

### Software and code

Policy information about [availability of computer code](#)

Data collection Flow cytometry data were acquired using SpectroFlo v.2.2 and SQS v.1.18.

Data analysis Flow cytometry data were analyzed using FlowJo v10 and Prism v9. ELISA, ELISpot, and neutralization data were analyzed using Prism v9. Sequence data were analyzed using Cell Ranger v.6.0.1, SCANPY v.1.7.2, pRESTO v0.6.2, IgBLAST v1.17.1, IMG/GENE-DB release 202113-2, Change-O v1.0.2, Alakazam v1.1.0, TIGER v1.0.0, circlize v.0.4.13, and SHazaM v1.0.2. VSV chimera neutralization data were analyzed using IN Cell Analyzer 1000 Workstation Software v3.7.

For manuscripts utilizing custom algorithms or software that are central to the research but not yet described in published literature, software must be made available to editors and reviewers. We strongly encourage code deposition in a community repository (e.g. GitHub). See the Nature Portfolio [guidelines for submitting code & software](#) for further information.

### Data

Policy information about [availability of data](#)

All manuscripts must include a [data availability statement](#). This statement should provide the following information, where applicable:

- Accession codes, unique identifiers, or web links for publicly available datasets
- A description of any restrictions on data availability
- For clinical datasets or third party data, please ensure that the statement adheres to our [policy](#)

Antibody sequences are deposited on GenBank under the following accession numbers: OQ634308 - OQ635939, available from GenBank/EMBL/DBJ. Newly reported raw sequencing data and transcriptomics count matrix are deposited at the Sequence Read Archive and Gene Expression Omnibus under BioProject PRJNA800176. Processed transcriptomics and BCR data are deposited at Zenodo (<https://doi.org/10.5281/zenodo.7719030>). Previously reported BCR data used in

this study were deposited under BioProjects PRJNA731610, PRJNA741267, and PRJNA777934. The IMGT/V-QUEST database is accessible at [http://www.imgt.org/IMGT\\_vquest/](http://www.imgt.org/IMGT_vquest/). Materials are available upon request, through an interinstitutional materials transfer agreement.

## Field-specific reporting

Please select the one below that is the best fit for your research. If you are not sure, read the appropriate sections before making your selection.

Life sciences  Behavioural & social sciences  Ecological, evolutionary & environmental sciences

For a reference copy of the document with all sections, see [nature.com/documents/nr-reporting-summary-flat.pdf](https://www.nature.com/documents/nr-reporting-summary-flat.pdf)

## Life sciences study design

All studies must disclose on these points even when the disclosure is negative.

Sample size	No statistical methods were used to determine sample size. 54 healthy participants were enrolled based on recruitment, of whom 54 provided peripheral blood, 25 provided axillary lymph node samples and 14 provided bone marrow samples. These numbers were sufficient to detect statistically significant differences in the effect sizes of interest.
Data exclusions	No data were excluded
Replication	Human samples were collected from 43 participants. ELISA and neutralization tests were performed once with two technical replicates. Affinity analysis via biolayer interferometry was performed at least two technical replicates according to the fitting-curve. ELISpot and flow cytometry experiments were performed once for each sample at each time point due to insufficient specimens. All attempts at replication were successful.
Randomization	Participants were from a sub-study of NCT04927065, which allocated them to different vaccine cohorts per its requirements. No other allocations to groups were made.
Blinding	No blinding was done for convenience; subjective measurements were not made.

## Reporting for specific materials, systems and methods

We require information from authors about some types of materials, experimental systems and methods used in many studies. Here, indicate whether each material, system or method listed is relevant to your study. If you are not sure if a list item applies to your research, read the appropriate section before selecting a response.

### Materials & experimental systems

n/a	Involved in the study
<input type="checkbox"/>	<input checked="" type="checkbox"/> Antibodies
<input type="checkbox"/>	<input checked="" type="checkbox"/> Eukaryotic cell lines
<input checked="" type="checkbox"/>	<input type="checkbox"/> Palaeontology and archaeology
<input checked="" type="checkbox"/>	<input type="checkbox"/> Animals and other organisms
<input type="checkbox"/>	<input checked="" type="checkbox"/> Human research participants
<input type="checkbox"/>	<input checked="" type="checkbox"/> Clinical data
<input checked="" type="checkbox"/>	<input type="checkbox"/> Dual use research of concern

### Methods

n/a	Involved in the study
<input checked="" type="checkbox"/>	<input type="checkbox"/> ChIP-seq
<input type="checkbox"/>	<input checked="" type="checkbox"/> Flow cytometry
<input checked="" type="checkbox"/>	<input type="checkbox"/> MRI-based neuroimaging

## Antibodies

### Antibodies used

total Ig (goat polyclonal, Jackson ImmunoResearch 109-005-064), IgG-HRP (goat polyclonal, Jackson ImmunoResearch 109-035-088), murine anti-S mAbs: SARS2-2, SARS2-11, SARS2-16, SARS2-31, SARS2-38, SARS2-57, and SARS2-71, SARS2-08, -09, -10, -13, -14, -17, -20, -26, -27, -28, -31, -41, -42, -44, -49, -62, -64, -65, and -67 (Diamond laboratory, Washington University School of Medicine), IgG (Sigma 12-349), IgG-BV480 (goat polyclonal, Jackson ImmunoResearch 109-685-098), PD-1-BB515 (EH12.1, BD Horizon 564494), IgA-FITC (M24A, Millipore CBL114F), CD45-A532 (HI30, Thermo 58-0459-42), Bcl6-PE (K112-91, 561522, BD Pharmingen), CD38-BB700 (HIT2, 566445, BD Horizon), Blimp1-PE (646702, IC36081P R&D), CD16 (3G8, 302002), CD32 (FUN-2, 303202), CD64 (10.1, 566178), CD19-BV421 (HIB19, 302234), FoxP3-BV421 (206D, 320129), CD20-Pacific Blue (2H7, 302320), CD27-BV510 (O323, 302836), CD8-BV570 (RPA-T8, 301038), IgM-BV-605 (MHM-88, 314524), HLA-DR-BV650 (L243, 307650), Ki-67-BV711 (Ki-67, 350516), CD19-BV750 (HIB19, 302262), CD3-FITC (HIT3a, 300306), CD71-FITC (CY1G4, 334104), IgD-PE (IA6-2, 348204), CD71-PE (CY1G4, 334106), CXCR5-PE-Dazzle 594 (J252D4, 356928), IgD-BV785 (IA6-2, 348242), CD4-PerCP (OKT4, 317432), CD14-PerCP (HCD14, 325632), IgD-PerCP-Cy5.5 (IA6-2, 348208), CD38-PE-Cy7 (HIT2, 303516), CD71-PE-Cy7 (CY1G4, 334112), CD19-APC (HIB19, 302212), CD4-Spark 685 (SK3, 344658), CD20-APC-Fire750 (2H7, 302358), CD3-APC-Fire810 (SK7, 344858); all Biologend.

### Validation

All commercial antibodies were validated by their manufacturers as detailed in their product information and titrated in the lab for the indicated assay by serial dilution. We validated mAbs generated in our lab in preliminary ELISAs and multiplex bead array to SARS-CoV-2 spike, bovine serum albumin, and anti-Ig. Influenza B/HA-specificity of mAb 321-05 6F05 was previously published (Turner, J. S. et al. Nature 586, 127–132 (2020)). E484-specificity of mAb mu 2B04 was previously published (Alsoussi, W. B. et al. J. Immunol. 205,



915–922 (2020)). S2-specificity of mAb 368-22 1B08 was previously published (Turner, J. S. et al. Nature 596, 109–113 (2021)).

## Eukaryotic cell lines

Policy information about [cell lines](#)

Cell line source(s)	Expi293F (Thermo), Vero E6 (ATCC), Vero-TMPRSS2 (Diamond Laboratory)
Authentication	The cell lines were not authenticated.
Mycoplasma contamination	Vero-TMPRSS2 lines are routinely tested each month and were negative for mycoplasma. Other cell lines were not tested for mycoplasma contamination. Growth rates were consistent with manufacturer's published data.
Commonly misidentified lines (See <a href="#">ICLAC</a> register)	No commonly misidentified cell lines were used.

## Human research participants

Policy information about [studies involving human research participants](#)

Population characteristics	Study participants demographics are detailed in Extended Data Table 1.
Recruitment	Study participants were recruited from the St. Louis metropolitan area by the Washington University Clinical Trials Unit. Potential self-selection and recruiting biases are unlikely to affect the parameters we measured.
Ethics oversight	The WU382 study was reviewed and approved by the Washington University Institutional Review Board (approval no. 202109021)

Note that full information on the approval of the study protocol must also be provided in the manuscript.

## Clinical data

Policy information about [clinical studies](#)

All manuscripts should comply with the ICMJE [guidelines for publication of clinical research](#) and a completed [CONSORT checklist](#) must be included with all submissions.

Clinical trial registration	NCT04927065
Study protocol	Details of protocol elements can be accessed from clinicaltrials.gov and Chalkias, S. et al. Nat. Med. 28, 2388–2397 (2022).
Data collection	Data for NCT04927065 from the subset of participants reported here were collected at the Washington University Infectious Disease Clinical Research Unit.
Outcomes	In this report of a subset of participants in the clinical trial, the following study primary endpoints are presented: Number of Participants with Solicited Local and Systemic Reactogenicity Adverse Reactions (Time Frame: 7 days post-vaccination, as recorded daily by participants). Number of Participants with Unsolicited Adverse Events (Time Frame: Up to 28 days post-vaccination).

## Flow Cytometry

### Plots

Confirm that:

- The axis labels state the marker and fluorochrome used (e.g. CD4-FITC).
- The axis scales are clearly visible. Include numbers along axes only for bottom left plot of group (a 'group' is an analysis of identical markers).
- All plots are contour plots with outliers or pseudocolor plots.
- A numerical value for number of cells or percentage (with statistics) is provided.

### Methodology

Sample preparation	Fine needle aspirates of axillary LNs were flushed from needles with 3 mL of RPMI supplemented with 10% FBS and 100 U/mL penicillin/streptomycin, followed by three 1 mL rinses. Red blood cells were lysed with ammonium chloride buffer, washed twice with PBS supplemented with 2% FBS, 2mM EDTA and immediately used or cryopreserved in 10% DMSO in FBS. Blood samples were collected in EDTA tubes, and peripheral blood mononuclear cells (PBMCs) were enriched by density gradient centrifugation over Ficoll 1077 (GE) or Lymphopure (BioLegend). The residual red blood cells were lysed with ammonium chloride lysis buffer, and cells were immediately used or cryopreserved in 10% dimethylsulfoxide in FBS.
Instrument	Cytek Aurora

- Software
- Cell population abundance
- Gating strategy
- Tick this box to confirm that a figure exemplifying the gating strategy is provided in the Supplementary Information.